THE PENNSYLVANIA STATE UNIVERSITY
SCHREYER HONORS COLLEGE

DEPARTMENT OF ELECTRICAL ENGINEERING

Modeling, Theory, and Simulation of Wideband Phased Array for Sensing and Communications

ANG CHEN
SUMMER 2022

A thesis
submitted in partial fulfillment
of the requirements
for a baccalaureate degree
in Electrical Engineering
with honors in Electrical Engineering

Reviewed and approved* by the following:

Wooram Lee
Associate Professor of Electrical Engineering
Thesis Supervisor

Julio Urbina
Associate Professor of Electrical Engineering
Honors Adviser

* Electronic approvals are on file.

ABSTRACT

The phased array is a key technology for Millimeter-Wave (mmWave) communication and sensing. The phased array consists of two or more antennas and features beamforming, beam steering, and beam tapering. With beamforming, the radiation pattern of a phased array can be narrowed to a concentrated beam compared to a single antenna. With beam steering, the phased array enables directional communications by controlling the phase difference of the individual antennas. And with beam tapering, the shape of the radiation pattern can be manipulated to suppress the power loss in the unwanted directions by altering the amplitude distribution of the individual antennas. In this thesis, fundamental features and principles of phased array antennas, including the configuration of phased array, array factor, beamforming, beam steering, grating lobes, and beam tapering, are explored and demonstrated using modeling, theoretical derivations, and MATLAB simulations.

TABLE OF CONTENTS

LIST OF FIGURES

LIST OF TABLES

ACKNOWLEDGEMENTS

With great gratitude, I acknowledge everyone who has inspired, mentored, and supported me throughout this independent research. First, I want to express my deepest appreciation to Dr. Wooram Lee, my Thesis Supervisor. As a distinguished expert in high-frequency integrated circuits and systems for communication and sensing, Dr. Lee helped me identify the research topic relevant to my interest, and offered me professional guidance in conducting the research and writing the thesis. Also, I could not have undertaken this journey without the tutelage of Dr. Julio Urbina, my Honors Advisor. Over the past two years, Dr. Urbina has provided me with valuable advice and challenged me to develop the characteristics and skills of a professional electrical engineer. Lastly, I would like to thank my family and friends for always encouraging me to strive for excellence.

Chapter 1

Introduction

1.1 Background of Telecommunication

Telecommunication technology has revolutionized the way human beings live. As technology advances every decade, telecommunication has gone through 1G, 2G, 3G, 4G, and 5G developments (Figure 1). With the advent of 1G, people could talk using cell phones. Using 2G, people could send and receive text messages. 3G enabled people to access the Internet through smartphones. With higher data transfer rates over 4G, people can do more with smartphones, such as watching online videos and playing online games. As more users come online and higher data-transfer rates are expected, 4G can barely meet the demand of soaring mobile data traffic. So, the fifth-generation telecommunication technology (5G) is currently being developed and becoming available to the public.

5G networks deliver ultra-high data speeds, ultra-low latency, and massive network capacity. The high speed of 5G will solve the problems caused by the explosive growth of mobile Internet traffic, and provide mobile Internet users with an enhanced application experience. With ultra-low latency, 5G can meet the needs of industries with extremely high requirements for latency and reliability, such as industrial control, telemedicine, and autonomous driving. 5G's massive network capacity will provide solutions for sensing and data collection applications, such as smart cities, smart homes, and environmental monitoring [1].

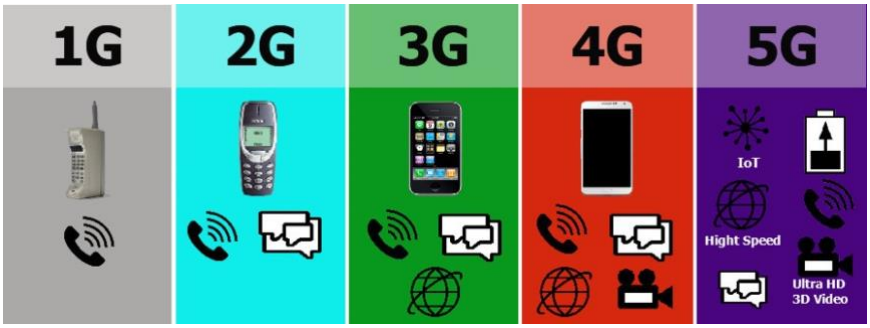

Figure 1. The Evolution of Telecommunication [1]

Despite its enormous potential, there are many challenges associated with 5G technology. Millimeter-Wave (mmWave) 5G networks are based on extremely high frequency (EHF) bands ranging from 30 GHz to 300 GHz. As data transfers at such high frequencies have very high path loss, mmWave 5G can be applied only on unobstructed and clear straight paths to the destination. In the real world, however, there are many obstacles between the transmitter and receiver, including buildings, cars, trees, mountains, and people, which makes mmWave 5G can only travel a short distance. Additionally, heavy attenuation from oxygen absorption and shadowing from obstacles at certain frequencies makes the short-range problem even more apparent (Table 1) [2][3].

Table 1. Advantages and Disadvantages of 5G Technology

Advantage	Disadvantage
Ultra-high data speed	Inability to penetrate blocking materials
Ultra-low latency	Heavy attenuation from oxygen absorption
Massive network capacity	

1.2 Realization of 5G Technology

Small cells with massive multiple-input multiple-output (MIMO) antennas can be used to overcome the short-range problem of 5G Technology.

A small cell is a portable miniature base station that uses minimal power and can be placed every 250 meters or so throughout cities. 5G signals can be prevented from being lost by installing thousands of small cells in a target area. 4G base stations have 12 antenna ports for cellular traffic: 8 for transmitters and 4 for receivers. 5G base stations can support about a hundred ports, which means more antennas can be arranged on a single array. By sending and receiving signals from many users simultaneously, a 5G MIMO base station can increase the capacity of mobile networks by a factor of 22 or greater. Installing many antennas to handle cellular traffic can also cause more interference if signal paths cross.

Beamforming can be implemented to resolve the interference problems. 5G base stations use beamforming to determine the most efficient route to deliver data to a particular user while reducing interference for nearby users. Rather than broadcasting in many directions, beamforming, focuses a signal on a concentrated beam that points exclusively at a user. The signal will have a better chance of arriving intact with this approach, and other signals will experience less interference (Figure 2) [4].

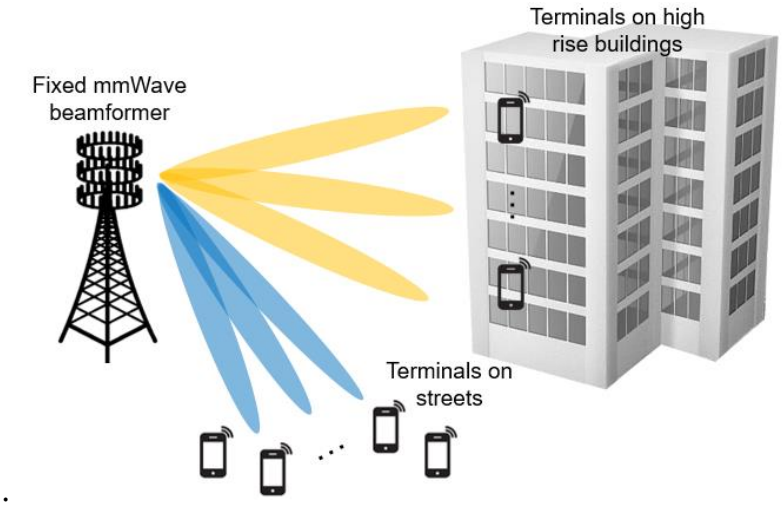

Figure 2. MmWave Beamformer Serving Mobile Terminals in MmWave 5G [5]

1.3 Motivation of Developing Phase Array

As beamforming can be realized with the phased array, the phased array becomes one of the key enabling technologies for mmWave communication and sensing. When two or more antennas are used, the combination is called an antenna array.

The radiation pattern of a phased array can be narrowed compared to a single antenna, which is beamforming. Also, combining multiple in-phase radiating elements results in higher radiation power than using a single radiating element. In addition, the phased-array system enables directional communications by controlling the phase difference of the individual antennas, which is beam steering. It also can produce multiple beams at the same time. Moreover, phased array antennas have lower cost and lower weight compared to single mechanically steering antennas. Compared with single antennas, phased array antennas are also much more reliable. If one antenna of the phased array fails, the remaining antennas will still function with slight changes to the radiation pattern [6].

Table 2. Advantages of Phased Array Technology

Advantages of Phased Array Technology		
Power	Beamforming	Beam Steering
Multi-Beams	Light Weight	Low Cost
Reliability		

Chapter 2

Array Factor

2.1 Configuration of Phased Array

The phased array can be divided into two categories based on the geometric configuration. It is called a linear array if all radiating elements are placed along a straight line (Figure 3). If all radiating elements are placed on a planar grid, it is called a planar array (Figure 4). The major difference between the two configurations is that a linear array can only electronically steer its beam within a single plane. In contrast, a planar array can steer the beam into two planes. In addition to two common phased arrays, there is another special phased array, the frequency scanning array, in which the transmitter's frequency controls the beam steering without using any phase shifter [7]. This thesis mainly focuses on the modeling, theory, and simulation of the properties and principles of the linear array with equal spacing between adjacent elements.

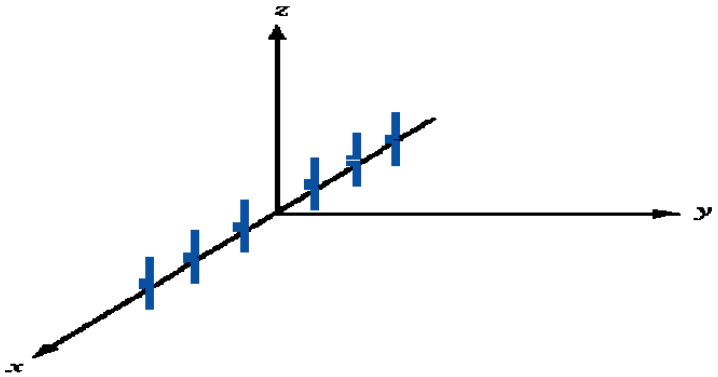

Figure 3. Linear Array Configuration [7]

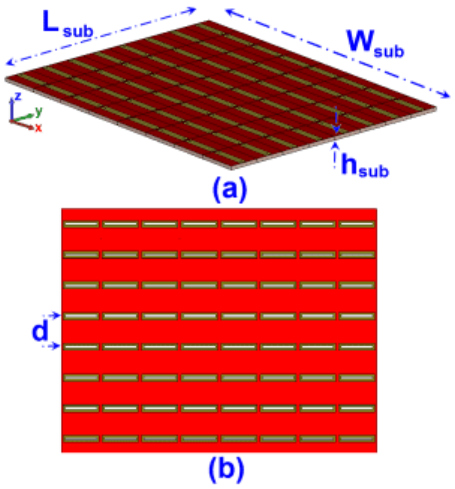

Figure 4. Planar Array Configuration: (a) Side View (b) Top View [7]

2.2 Single Radiating Element

Before considering the linear phased array, a single radiating element in the far-field region will be firstly introduced. The far-field region exists when

$$R > \frac{2D^2}{\lambda}$$

where R is the distance from the antenna, D is the maximum linear dimension of the antenna, and λ is the wavelength [8].

In the far-field region, the electromagnetic wave propagates much like a plane. Therefore, the radiation patterns are independent of the distance from the antenna. In the spherical coordinate system, the electric field intensity $\tilde{E}(R, \theta, \phi)$ of a single radiating element is the production of the spherical propagation factor $\frac{e^{-jkR}}{R}$, which is only related to the distance R, and the directional dependence function $\tilde{f}_e(\theta, \phi)$:

$$\tilde{E}_e(R, \theta, \phi) = \frac{e^{-jkR}}{R} \tilde{f}_e(\theta, \phi)$$

where k is the wavelength, and the power density S_e can be expressed as

$$S_e(R,\theta,\phi) = \frac{1}{2\eta_0}\left|\tilde{E}_e(R,\theta,\phi)\right|^2 = \frac{1}{2\eta_0}\left|\frac{e^{-jkR}}{R}\tilde{f}_e(\theta,\phi)\right|^2 = \frac{1}{2\eta_0 R^2}\left|\tilde{f}_e(\theta,\phi)\right|^2$$

2.3 Linear Array Configuration

Then we begin to set up a one-dimensional linear array configuration. N identical radiating elements are aligned among the z-axis from $z = 0$ towards the positive z-direction with equal spacing d between adjacent elements. Elements are named from "element 0" to "element $N-1$."

All antenna elements are fed by a common oscillator. And each antenna element is controlled by a phase shifter ψ_i and an amplifier (or attenuator) a_i on its corresponding transmission line. Q is the observation point in the far-field region, and its position is (R_0, θ, ϕ) (Figure 5).

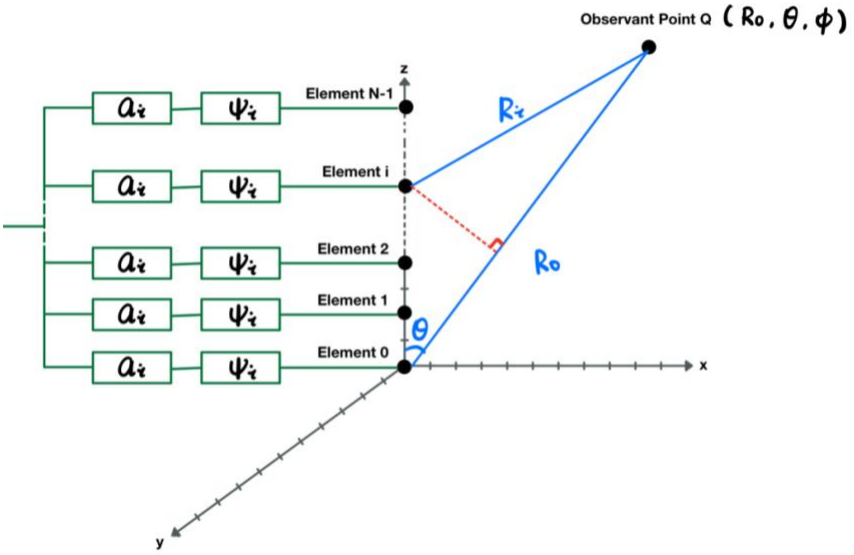

Figure 5. Linear Array Layout and Setting Used in This Thesis

To meet the far-field condition,

$$R_0 > \frac{2D^2}{\lambda} = \frac{2[(N-1)d^2]^2}{\lambda} = \frac{2(N-1)^2 d^2}{\lambda}$$

At Q, the electric field intensity due to element i is

$$\tilde{E}_e(R_i, \theta, \phi) = A_i \frac{e^{-jkR_i}}{R_i} \tilde{f}_e(\theta, \phi)$$

where A_i is the complex feeding coefficient due to the excitation by the phase shifter ψ_i and the amplifier (or attenuator) a_i, which can be expressed as

$$A_i = a_i e^{j\psi_i}$$

The total electric field intensity at Q is the summation of the electric field intensity due to each single antenna element, which is

$$\tilde{E}(R_0, \theta, \phi) = \sum_{i=0}^{N-1} \tilde{E}_e(R_i, \theta, \phi) = \tilde{f}_e(\theta, \phi) \sum_{i=0}^{N-1} A_i \frac{e^{-jkR_i}}{R_i}$$

Since the spacing between each adjacent element is d, the distance from element 0 to element i is id. By the trigonometric theorem and under the far-field condition,

$$R_0 \approx R_i + id\cos\theta$$

$$R_i \approx R_0 - id\cos\theta$$

By replacing R_i in the denominator with R_0 and replacing R_i in the exponential part with $R_0 - id\cos\theta$, the expression of total electric field intensity at Q becomes

$$\tilde{E}(R_0, \theta, \phi) = \tilde{f}_e(\theta, \phi) \sum_{i=0}^{N-1} A_i \frac{e^{-jk(R_0 - id\cos\theta)}}{R_0} = \frac{e^{-jkR_0}}{R_0} \tilde{f}_e(\theta, \phi) \sum_{i=0}^{N-1} A_i \, e^{jikd\cos\theta}$$

and the power density of the phased array is

$$S(R_0, \theta, \phi) = \frac{1}{2\eta_0} \left|\tilde{E}(R_0, \theta, \phi)\right|^2 = \frac{1}{2\eta_0} \left| \frac{e^{-jkR_0}}{R_0} \tilde{f}_e(\theta, \phi) \sum_{i=0}^{N-1} A_i \, e^{jikd\cos\theta} \right|^2$$

$$= \frac{1}{2\eta_0 {R_0}^2} \left|\tilde{f}_e(\theta, \phi)\right|^2 \left| \sum_{i=0}^{N-1} A_i \, e^{jikd\cos\theta} \right|^2 = S_e(R, \theta, \phi) \left| \sum_{i=0}^{N-1} A_i \, e^{jikd\cos\theta} \right|^2$$

2.4 Derivation of Array Factor

From the above equation, the power density of a linear array with equal spacing between adjacent elements is the product of the power density of a single antenna element, $S_e(R,\theta,\phi)$, and $\left|\sum_{i=0}^{N-1} A_i\, e^{jikd\cos\theta}\right|^2$, which is defined as the array factor $F_a(\theta)$. The array factor $F_a(\theta)$ is a function of the positions of the individual radiating elements and their feeding coefficients. It is irrelative to the types of antenna elements. Then the power density of the phased array can be expressed as

$$S(R_0,\theta,\phi) = S_e(R,\theta,\phi)F_a(\theta)$$

which demonstrates the pattern multiplication principle.

To calculate the power density of a phased array, we can calculate the array factor $F_a(\theta)$ by replacing all antenna elements with isotropic radiating elements, then multiply the power density of a single antenna element $S_e(R,\theta,\phi)$. From the equation for the array factor $F_a(\theta)$,

$$F_a(\theta) = \left|\sum_{i=0}^{N-1} A_i\, e^{jikd\cos\theta}\right|^2 = \left|\sum_{i=0}^{N-1} a_i e^{j\psi_i}\, e^{jikd\cos\theta}\right|^2$$

we can tell that the array factor $F_a(\theta)$ is controlled by the array amplitude distribution a_i and the array phase distribution ψ_i.

By altering ψ_i, we can change the direction of the radiation pattern, which is beam steering. By altering a_i, we can control the shape of the radiation pattern to suppress the power loss in the unwanted direction, which is beam tapering.

In the next few chapters, the derivation of mathematical equations and MATLAB simulations will be used to find the properties of beamforming, beam steering, and beam tapering, providing fundamental principles to design phased array antennas.

Chapter 3

Beamforming

3.1 Radiation Pattern of a Single Radiating Element

5G and its real-world implementation require the use of beamforming technology. One of the advantages of the phased array is beamforming. Since the power density of the phased array is the multiplication of the power density of a single radiating element $S_e(R,\theta,\phi)$ and the array factor $F_a(\theta)$, if all radiating elements are identical and isotropic, the radiation pattern of such a phased array refers to the directional (angular) dependence of the strength of the array factor $F_a(\theta)$. From

$$F_a(\theta) = \left|\sum_{i=0}^{N-1} A_i\, e^{jikd\cos\theta}\right|^2 = \left|\sum_{i=0}^{N-1} a_i e^{j\psi_i}\, e^{jikd\cos\theta}\right|^2$$

and

$$k = \frac{2\pi}{\lambda} = \frac{2\pi}{\frac{c}{f}} = \frac{2\pi f}{c}$$

we can get

$$F_a(\theta) = \left|\sum_{i=0}^{N-1} A_i\, e^{jikd\cos\theta}\right|^2 = \left|\sum_{i=0}^{N-1} a_i e^{j\psi_i}\, e^{ji\frac{2\pi f}{c}d\cos\theta}\right|^2$$

The above equation shows that the array factor $F_a(\theta)$ is a function of θ, which depends on the five parameters: the number of radiating elements N, the phase shifter ψ_i, the amplifier a_i, the frequency f, and the distance between adjacent radiating elements d. The radiation pattern will change by changing any of the above parameters.

For a single isotropic element, it propagates in all directions with the same strength. So, the radiation pattern simulated by MATLAB (Appendix A) is a horizontal line, as shown in Figure 6.

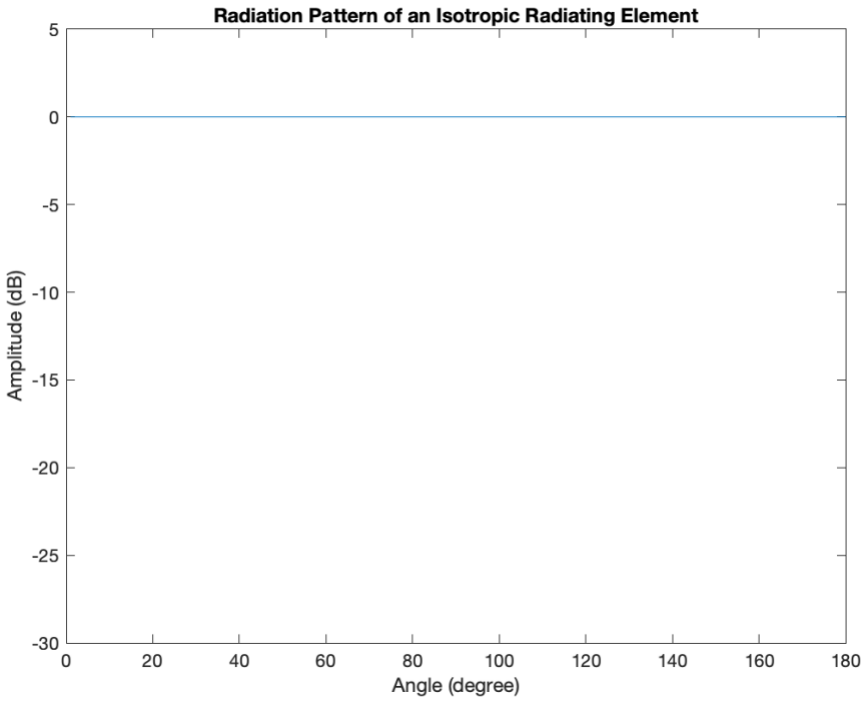

Figure 6. Radiation Pattern of An Isotropic Radiating Element

3.2 Radiation Pattern of Linear Array with Uniform Distribution

If each antenna of a linear array has an equal phase distribution, ψ_i=ψ_0, then

$$F_a(\theta) = \left|\sum_{i=0}^{N-1} a_i e^{j\psi_0}\, e^{jikd\cos\theta}\right|^2 = \left|e^{j\psi_0}\right|^2 \left|\sum_{i=0}^{N-1} a_i\, e^{jikd\cos\theta}\right|^2 = \left|\sum_{i=0}^{N-1} a_i\, e^{jikd\cos\theta}\right|^2$$

The phased difference between the fields radiated by adjacent elements is defined as

$$\gamma = kd\cos\theta = \frac{2\pi d}{\lambda}\cos\theta = \frac{2\pi f d}{c}\cos\theta$$

So,

$$F_a(\gamma) = \left|\sum_{i=0}^{N-1} a_i\, e^{ji\gamma}\right|^2$$

If each antenna has the equal amplitude distribution, $a_i = 1$, and equal phase distribution, ψ_i=ψ_0, then

$$F_a(\gamma) = \left|\sum_{i=0}^{N-1} e^{ji\gamma}\right|^2 = \left|1 + e^{j\gamma} + e^{j2\gamma} + \cdots + e^{j(N-1)\gamma}\right|^2$$

From the above equation, we can figure out that the maximum value of the array factor $F_a(\gamma)$ is approached when $\gamma = 0$,

$$F_a(\gamma)_{max} = F_a(0) = \left|\sum_{i=0}^{N-1} e^0\right|^2 = |N|^2 = N^2$$

In this situation,

$$\gamma = kd\cos\theta = 0$$

$$\cos\theta = 0$$

$$\theta = \frac{\pi}{2}$$

From here, we can conclude that the main beam of the radiation pattern of linear arrays with uniform amplitude and phase distribution is always perpendicular to the lines formed by radiating elements. Such arrays are broadside arrays.

To virtualize the radiation pattern of a linear array and to verify that the maximum value of the array factor $F_a(\gamma)$ is approached when $\theta = \frac{\pi}{2}$, we then simulate the radiation pattern by MATLAB (Appendix A). Setting that the number of radiating elements N is 2, the frequency f is 28 GHz, and the distance between adjacent elements d is $\frac{\lambda}{2}$, the radiation pattern is shown in Figure 7.

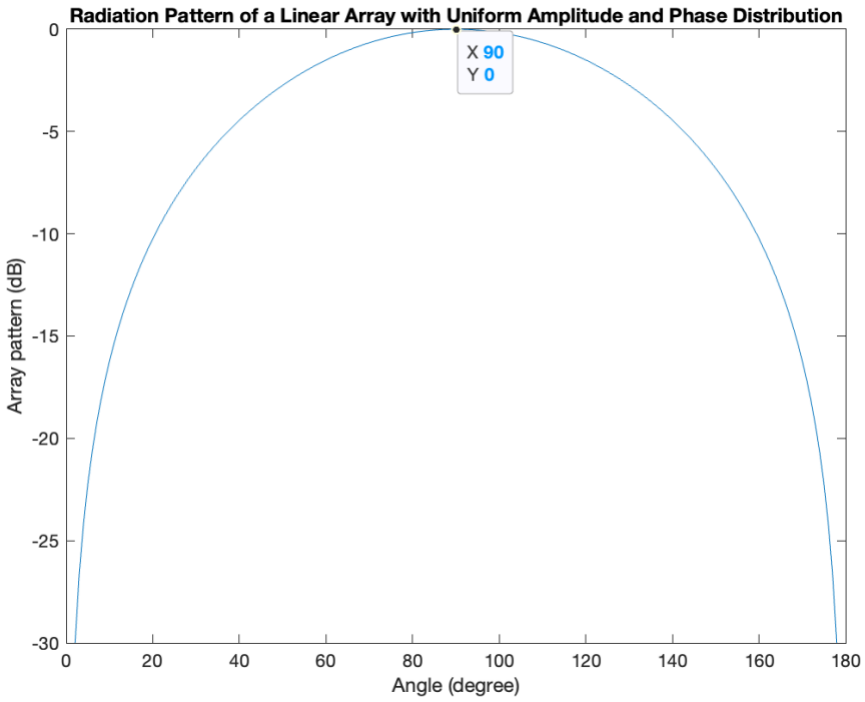

Figure 7. Radiation Pattern Simulated by Original Equation for Array Factor

From Figure 7, it is now verified that the maximum value of the array factor $F_a(\gamma)$ is approached when $\theta = \frac{\pi}{2}$. Furthermore, by comparing Figure 6 and Figure 7, the linear array indeed has the feature of beamforming.

We now continue simplifying the equation for array factor with some mathematical derivations. Let

$$f_a(\gamma) = 1 + e^{j\gamma} + e^{j2\gamma} + \cdots + e^{j(N-1)\gamma}$$

then

$$F_a(\gamma) = \left|1 + e^{j\gamma} + e^{j2\gamma} + \cdots + e^{j(N-1)\gamma}\right|^2$$

$$F_a(\gamma) = |f_a(\gamma)|^2$$

We have

$$f_a(\gamma) = 1 + e^{j\gamma} + e^{j2\gamma} + \cdots + e^{j(N-1)\gamma} \quad (1)$$

$$f_a(\gamma)e^{j\gamma} = \left(1 + e^{j\gamma} + e^{j2\gamma} + \cdots + e^{j(N-1)\gamma}\right)e^{j\gamma}$$

$$f_a(\gamma)e^{j\gamma} = e^{j\gamma} + e^{j2\gamma} + \cdots + e^{jN\gamma} \quad (2)$$

The difference between (1) and (2) is

$$f_a(\gamma)(1 - e^{j\gamma}) = 1 - e^{jN\gamma}$$

So,

$$f_a(\gamma) = \frac{1 - e^{jN\gamma}}{1 - e^{j\gamma}} = \frac{e^{\frac{jN\gamma}{2}}}{e^{\frac{j\gamma}{2}}}\left(\frac{e^{-\frac{jN\gamma}{2}} - e^{\frac{jN\gamma}{2}}}{e^{-\frac{j\gamma}{2}} - e^{\frac{j\gamma}{2}}}\right) = \frac{e^{\frac{jN\gamma}{2}}}{e^{\frac{j\gamma}{2}}}\left(\frac{sin\left(\frac{N\gamma}{2}\right)}{sin\left(\frac{\gamma}{2}\right)}\right) = e^{\frac{j(N-1)\gamma}{2}}\left(\frac{sin\left(\frac{N\gamma}{2}\right)}{sin\left(\frac{\gamma}{2}\right)}\right)$$

Then,

$$F_a(\gamma) = |f_a(\gamma)|^2 = f_a(\gamma) \cdot f_a(\gamma)^* = e^{\frac{j(N-1)\gamma}{2}}\left(\frac{sin\left(\frac{N\gamma}{2}\right)}{sin\left(\frac{\gamma}{2}\right)}\right) * e^{\frac{-j(N-1)\gamma}{2}}\left(\frac{sin\left(\frac{N\gamma}{2}\right)}{sin\left(\frac{\gamma}{2}\right)}\right) = \frac{sin^2(\frac{N\gamma}{2})}{sin^2(\frac{\gamma}{2})}$$

Finally,

$$F_a(\gamma) = \frac{sin^2(\frac{N\gamma}{2})}{sin^2(\frac{\gamma}{2})}$$

In the previous content, we know that the maximum value of the array factor $F_a(\gamma)$ is N^2 when $\theta = \frac{\pi}{2}$. The normalized array factor is the ratio of the array factor $F_a(\gamma)$ to the maximum value of the array factor N^2, which is

$$F_{a\_norm}(\gamma) = \frac{sin^2(\frac{N\gamma}{2})}{N^2 sin^2(\frac{\gamma}{2})} = \frac{sin^2(\frac{N\pi d}{\lambda}cos\theta)}{N^2 sin^2(\frac{\pi d}{\lambda}cos\theta)}$$

or

$$F_{a\_norm}(\theta) = \frac{sin^2(\frac{N\pi d}{\lambda}cos\theta)}{N^2 sin^2(\frac{\pi d}{\lambda}cos\theta)}$$

To verify the correctness of the above simplification of the equation for the array factor and the equation for the normalized array factor, we implement both into MATLAB (Appendix A). Setting that the number of radiating elements N is 2, the frequency f is 28 GHz, and the distance between adjacent elements d is $\frac{\lambda}{2}$, the radiation pattern of applying the equation for the simplified normalized array factor is shown in Figure 8.

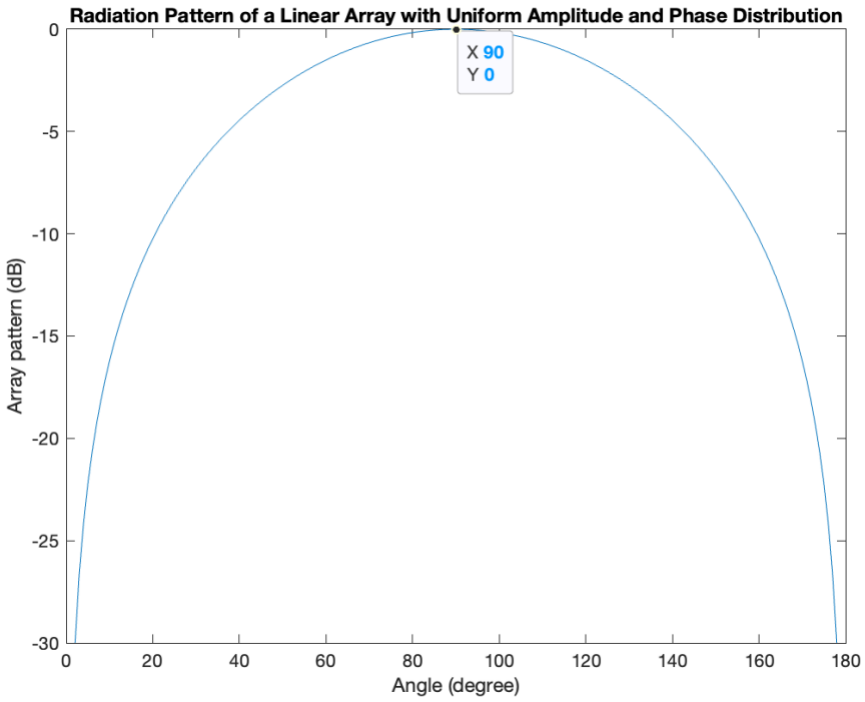

Figure 8. Radiation Pattern Simulated by Equation for Normalized Array Factor

By comparing Figure 7 and Figure 8, we find that the two graphs are identical. Therefore, the simplified equation for the array factor and the simplified equation for the normalized array factor are correct.

We now explore the effect on the radiation pattern if changing the number of elements N in MATLAB (Appendix A). Suppose the frequency f is 28 GHz, the distance between adjacent elements d is $\frac{\lambda}{2}$, and the number of radiating elements N changes from 4, 8, 16, and 32. The radiation pattern is shown in Figure 9, Figure 10, Figure 11, and Figure 12.

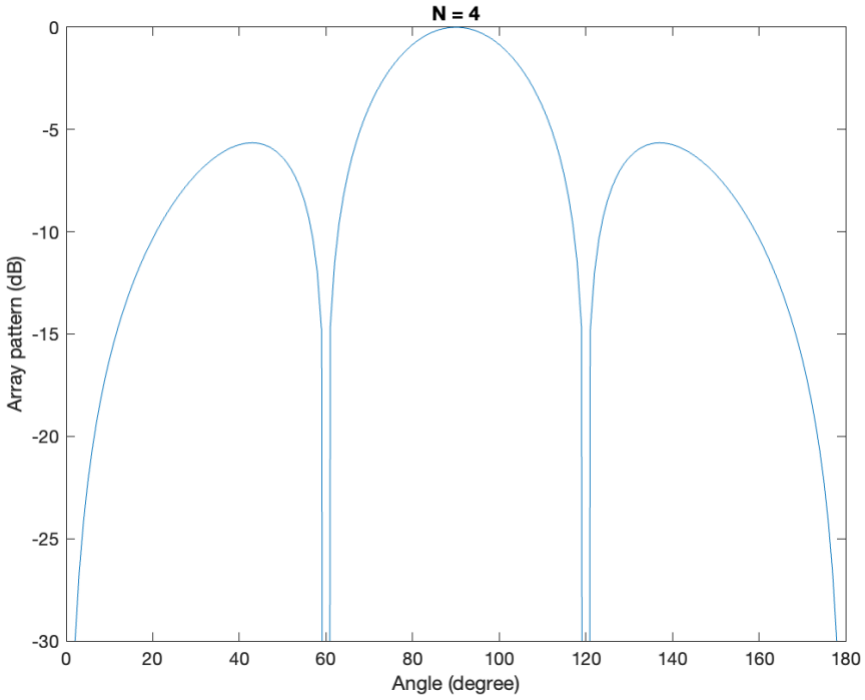

Figure 9. N = 4

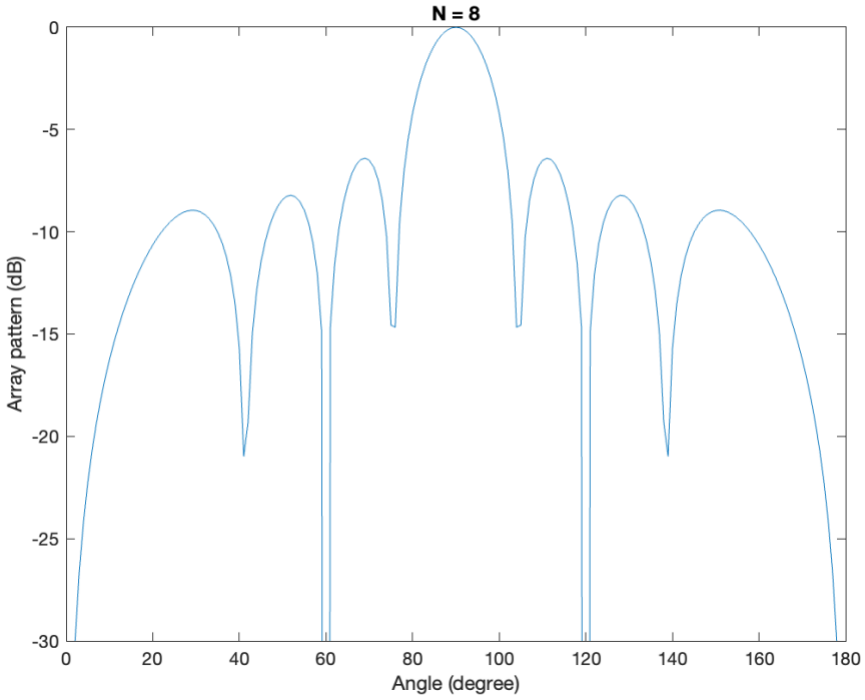

Figure 10. N = 8

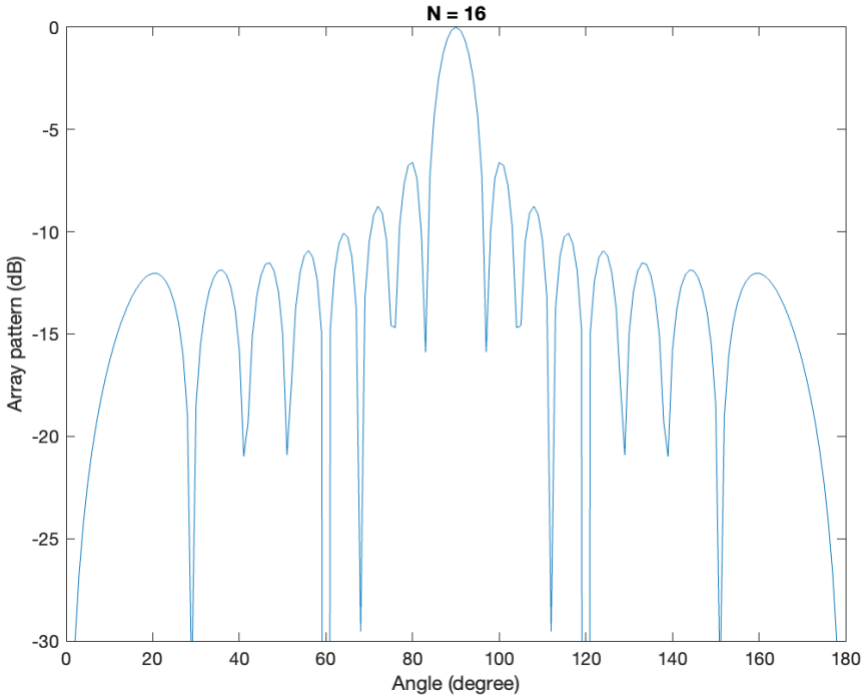

Figure 11. N = 16

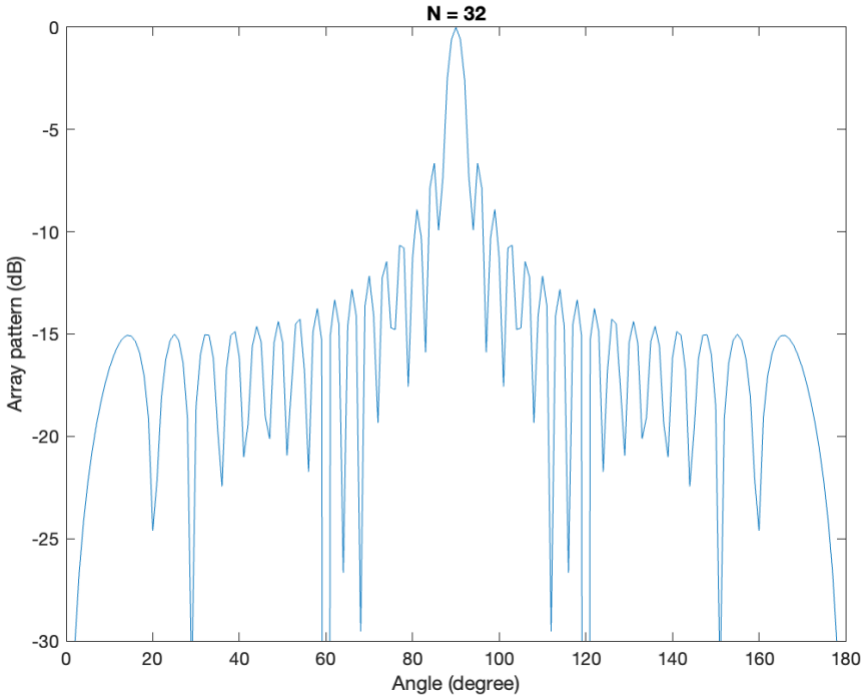

Figure 12. N = 32

The above figures show that when the number of elements *N* increases, the beamwidth of the main lobe decreases. So, the array directivity towards the main lobe increases.

3.3 Multiple Beams

Suppose the number of radiating elements N is still 2. The frequency f is still 28 GHz. And the distance between adjacent elements d changes from $\frac{\lambda}{2}$, to $3 \cdot \frac{\lambda}{2}$, to $5 \cdot \frac{\lambda}{2}$, to $7 \cdot \frac{\lambda}{2}$. By MATLAB Simulation (Appendix A). The radiation pattern of $\frac{\lambda}{2}$ is shown in Figure 13. The radiation pattern of $3 \cdot \frac{\lambda}{2}$ is shown in Figure 14. The radiation pattern of $5 \cdot \frac{\lambda}{2}$ is shown in Figure 15. The radiation pattern of $7 \cdot \frac{\lambda}{2}$ is shown in Figure 16.

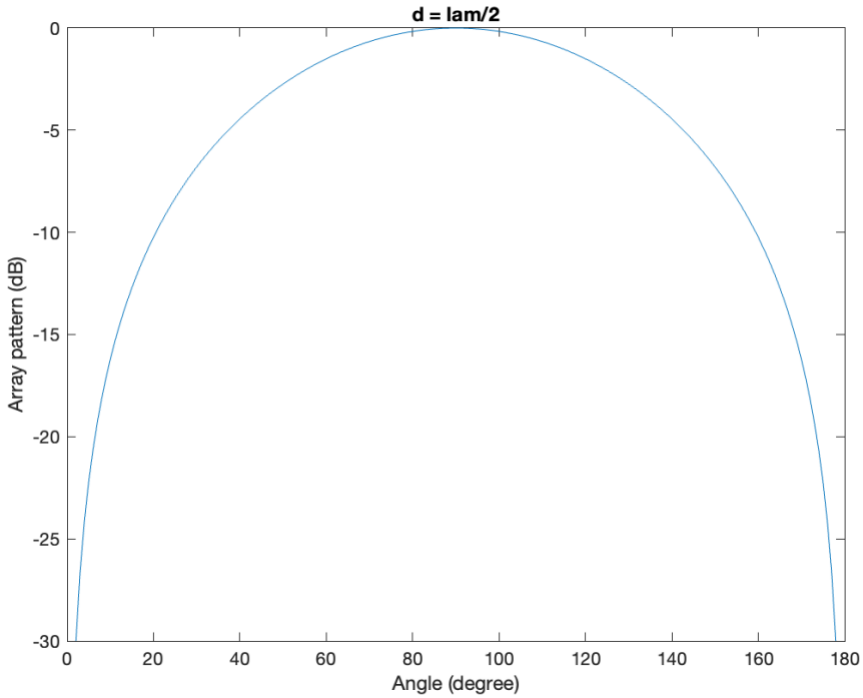

Figure 13. d = λ/2

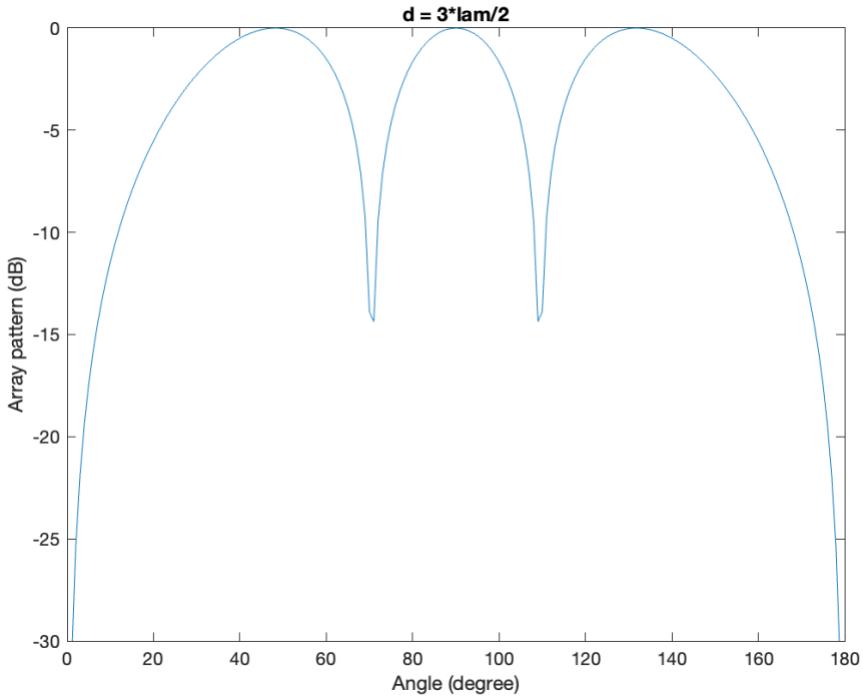

Figure 14. d = 3λ/2

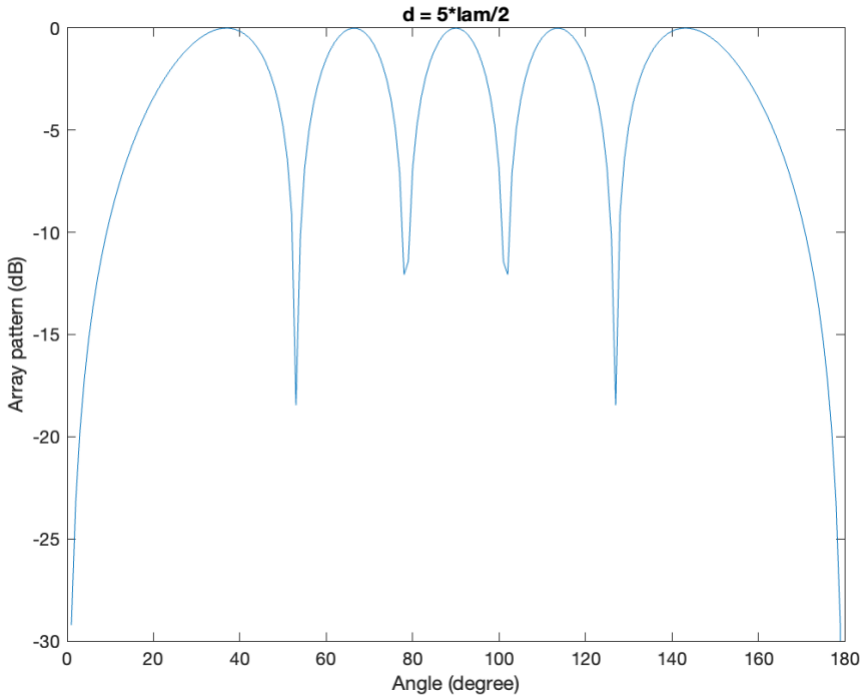

Figure 15. d = 5λ/2

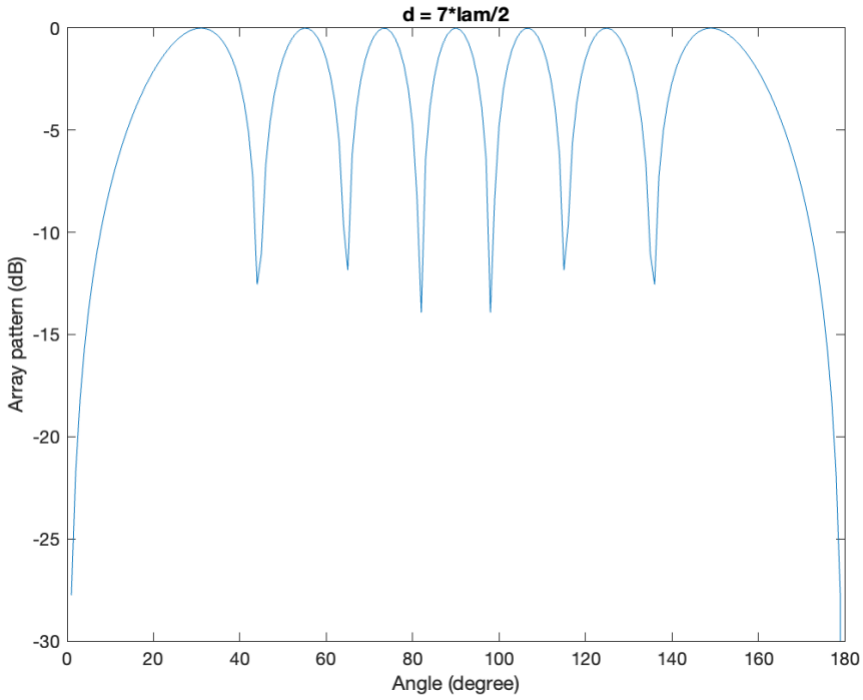

Figure 16. d = 7λ/2

By comparing the above figures, we find that the phased array produces multiple beams with the same peak value. When d is $\frac{\lambda}{2}$, there is one beam. When d is $3 \cdot \frac{\lambda}{2}$, there are three beams. When d is $5 \cdot \frac{\lambda}{2}$, there are five beams. When d is $7 \cdot \frac{\lambda}{2}$, there are seven beams.

Table 3. Relationship Between Element Spacing and Number of Beams

Distance Between Adjacent Elements	Number of Beams
$\frac{\lambda}{2}$	1
$3 \cdot \frac{\lambda}{2}$	3
$5 \cdot \frac{\lambda}{2}$	5
$7 \cdot \frac{\lambda}{2}$	7

In conclusion, as d increases, the number of beams also increases while the beamwidth of each beam decreases. In addition, the number of beams between $0^{\circ}$and 180° equals $d\ /\frac{\lambda}{2}$. The mathematical derivation of multiple beams is demonstrated in Chapter 5.2.

Chapter 4

Beam Steering

Beam steering is another major property of the phased array. By changing the phase distribution, the direction of the radiation pattern can be altered from the broadside to any direction we want. Beam steering eliminates the need to mechanically steer an antenna and increases the steering rate.

Assume we apply a linear phase distribution, $\psi_i = -i\delta$, to an antenna array, where δ is the incremental phase delay between adjacent elements, as shown in Figure 17.

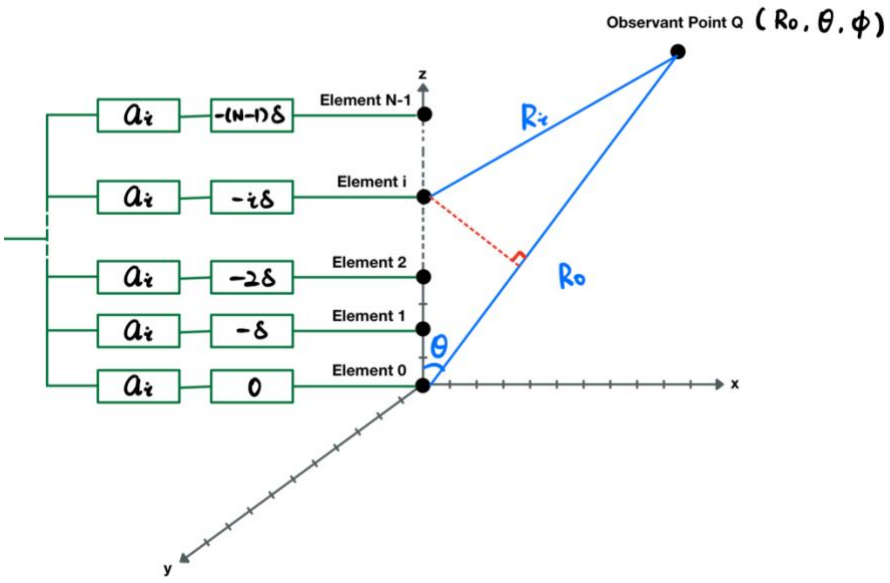

Figure 17. Configuration of Linear Phase Distribution

Then the array factor $F_a(\theta)$ becomes

$$F_a(\theta) = \left|\sum_{i=0}^{N-1} a_i e^{-ji\delta}\, e^{jikd\cos\theta}\right|^2 = \left|\sum_{i=0}^{N-1} a_i\, e^{ji(kd\cos\theta-\delta)}\right|^2$$

The phased difference between the fields radiated by adjacent elements is

$$\gamma' = kd\cos\theta - \delta$$

Then,

$$F_a(\gamma') = \left| \sum_{i=0}^{N-1} a_i \, e^{ji\gamma'} \right|^2$$

Since the array factor equation for the linear phase distribution is the same as for the uniform phase distribution except for the difference between γ and γ', the array factor of a linear phase distribution can always be obtained from the array factor of a uniform phase distribution by changing γ to γ', regardless of the amplitude distribution.

Under the condition that the amplitude distribution is symmetrical with the array center [8], the array factor $F_a(\gamma')$ is maximum when

$$\gamma' = 0$$

$$kd\cos\theta - \delta = 0$$

If we set $\delta = kd\cos\theta_0$, then the array factor $F_a(\gamma')$ is maximum when

$$kd\cos\theta - kd\cos\theta_0 = 0$$

$$kd(\cos\theta - \cos\theta_0) = 0$$

$$\cos\theta - \cos\theta_0 = 0$$

$$\theta = \theta_0$$

So, by applying a linear phase distribution, we steer the direction of the maximum radiation (main lobe) from the broadside direction to θ_0, which is the scan angle. To steer the beam to the end-fire direction ($\theta_0 = 0$), the incremental phase shift

$$\delta = kd\cos\theta_0 = kd\cos(0) = kd$$

To verify the correctness, we simulate it by MATLAB (Appendix B). Suppose that the number of radiating elements N is 8, the frequency f is 28 GHz, the distance between adjacent elements d is $\frac{\lambda}{2}$, and the amplitude distribution is uniform. The radiation pattern of applying $F_a(\theta) = \left|\sum_{i=0}^{N-1} a_i \, e^{ji(kd\cos\theta - \delta)}\right|^2$ by setting θ_0 to 0°, 30°, 60°, 90°, 120°, and 150° is shown in Figure 18, Figure 19, Figure 20, Figure 21, Figure 22, and Figure 23.

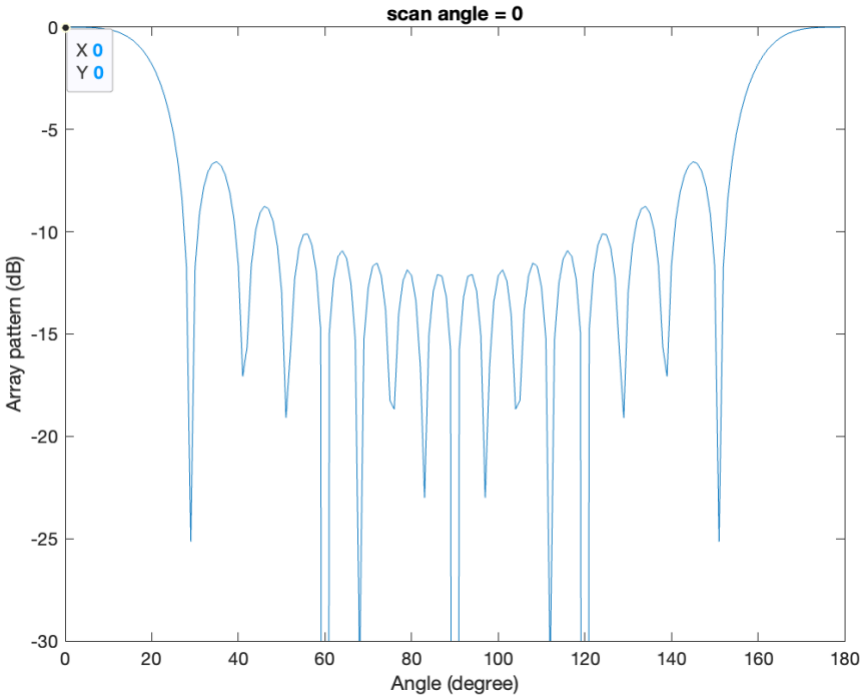

Figure 18. Scan Angle = 0

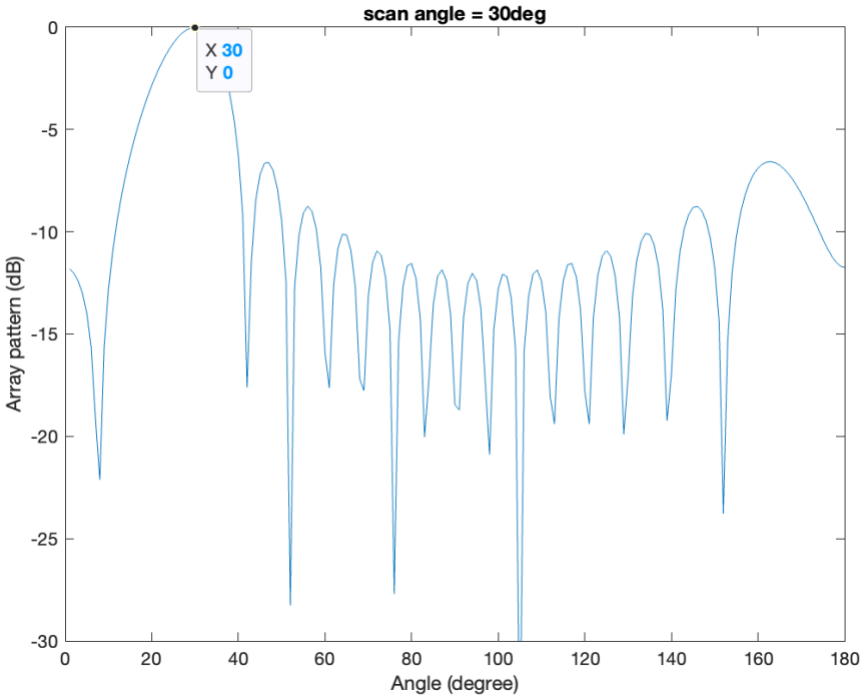

Figure 19. Scan Angle = 30°

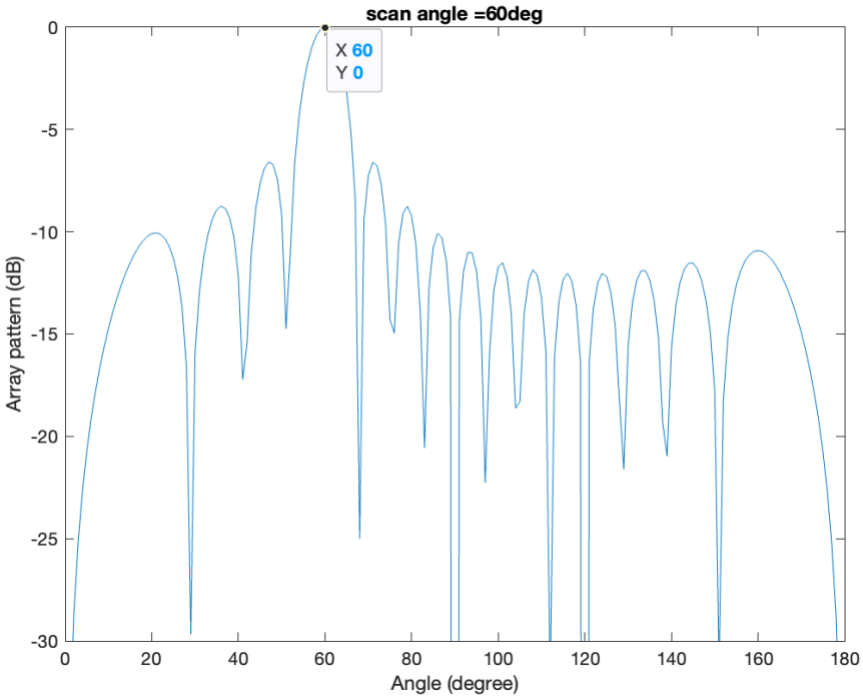

Figure 20. Scan Angle = 60°

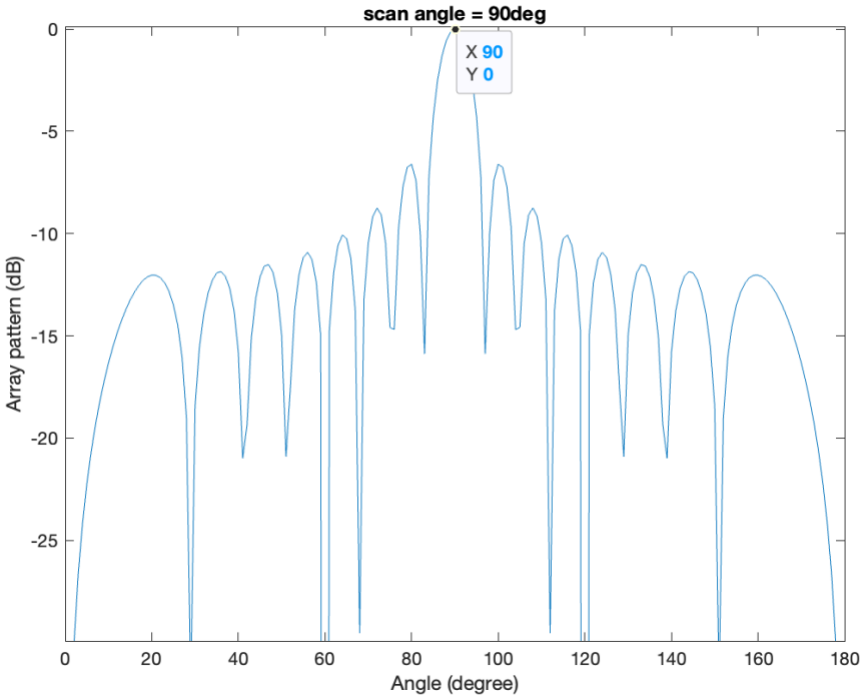

Figure 21. Scan Angle = 90°

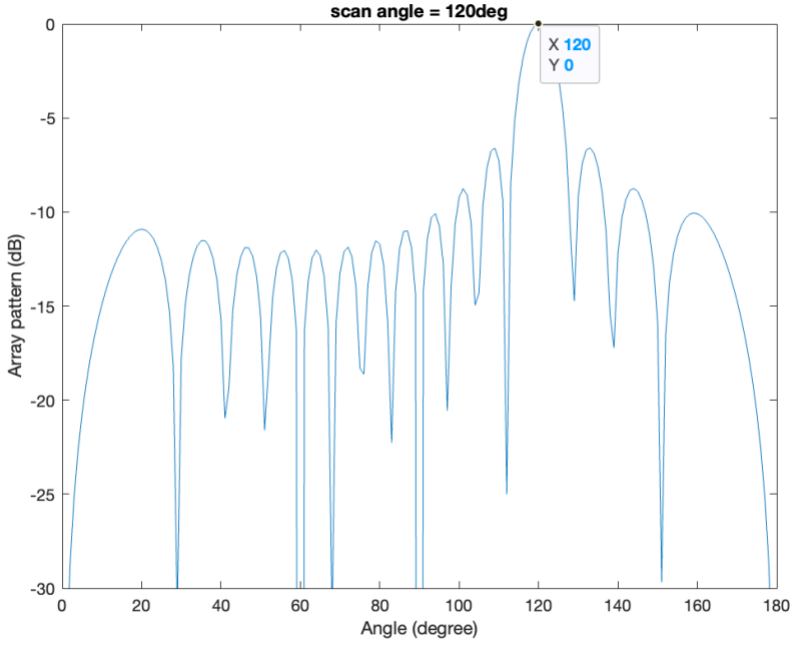

Figure 22. Scan Angle = 120°

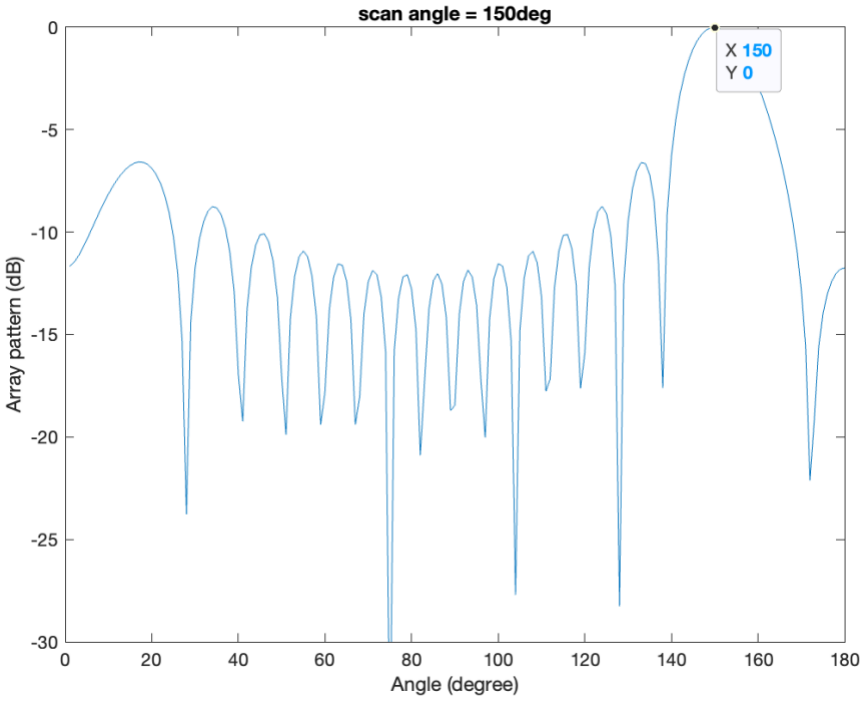

Figure 23. Scan Angle = 150°

Based on the above figures, we confirm that the MATLAB simulation matches the expectation. So, to alter the direction of the radiation pattern of a phased array towards an angle θ_0, we could apply a linear phase distribution

$$\psi_i = -i\delta = -ikd\cos\theta_0$$

to achieve this goal.

Furthermore, if the linear array has linear phase distribution and uniform amplitude distribution, then the normalized array factor is the ratio of the array factor $F_a(\gamma')$ to the maximum value of the array factor N^2, which is

$$F_{a\_norm}(\gamma') = \frac{sin^2(\frac{N\gamma'}{2})}{N^2 sin^2(\frac{\gamma'}{2})} = \frac{sin^2[\frac{N\pi d}{\lambda}(cos\theta - cos\theta_0)]}{N^2 sin^2[\frac{\pi d}{\lambda}(cos\theta - cos\theta_0)]}$$

Chapter 5

Grating Lobes

5.1 Simulation of Grating Lobes

In the previous simulation, we assume that the distance between adjacent radiating elements d equals $\frac{\lambda}{2}$. Further MATLAB simulation (Appendix C) is performed to explore how radiation pattern changes as altering d. Suppose that the number of radiating elements N is 16, the frequency f is 28 GHz, and the amplitude and phase distribution is uniform. The radiation pattern of applying $F_a(\theta) = \left|\sum_{i=0}^{N-1} e^{ji(kd\cos\theta)}\right|^2$ by changing the distance between adjacent radiating elements d to 0.25λ, 0.5λ, 0.75λ, λ, 1.25λ is shown in Figure 24, Figure 25, Figure 26, Figure 27, and Figure 28.

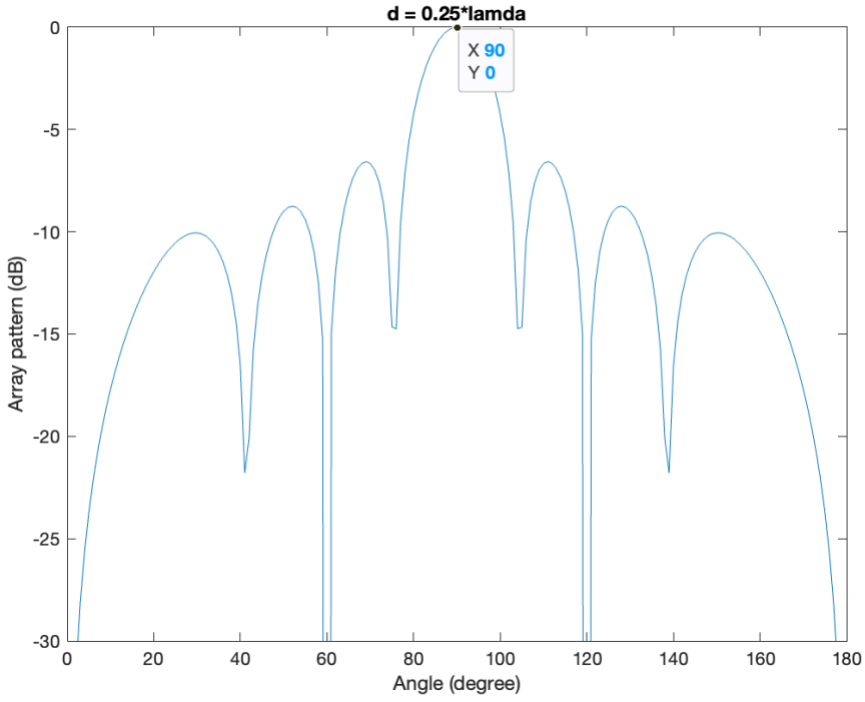

Figure 24. d = 0.25λ, Scan Angle = 90°

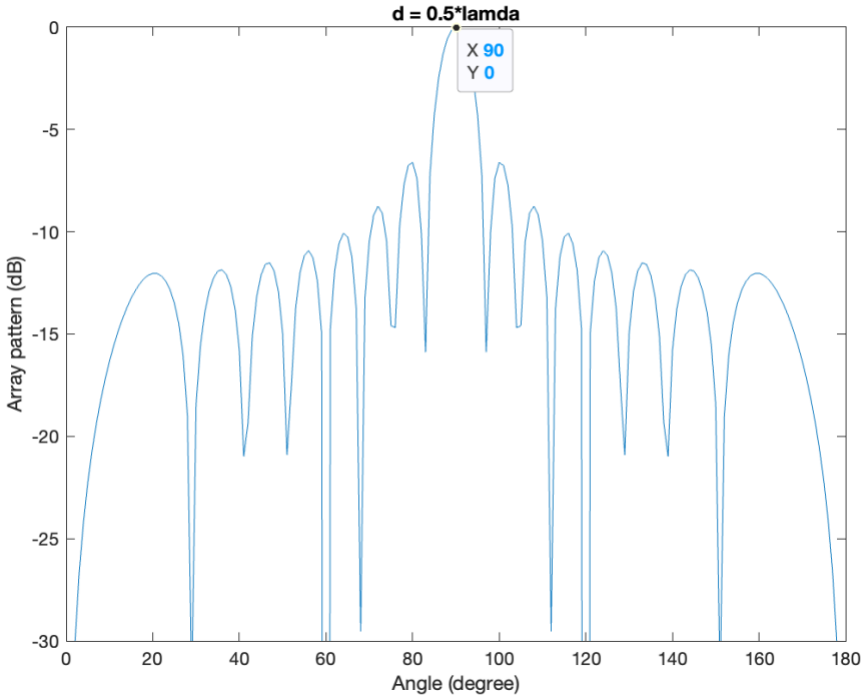

Figure 25. d = 0.5λ, Scan Angle = 90°

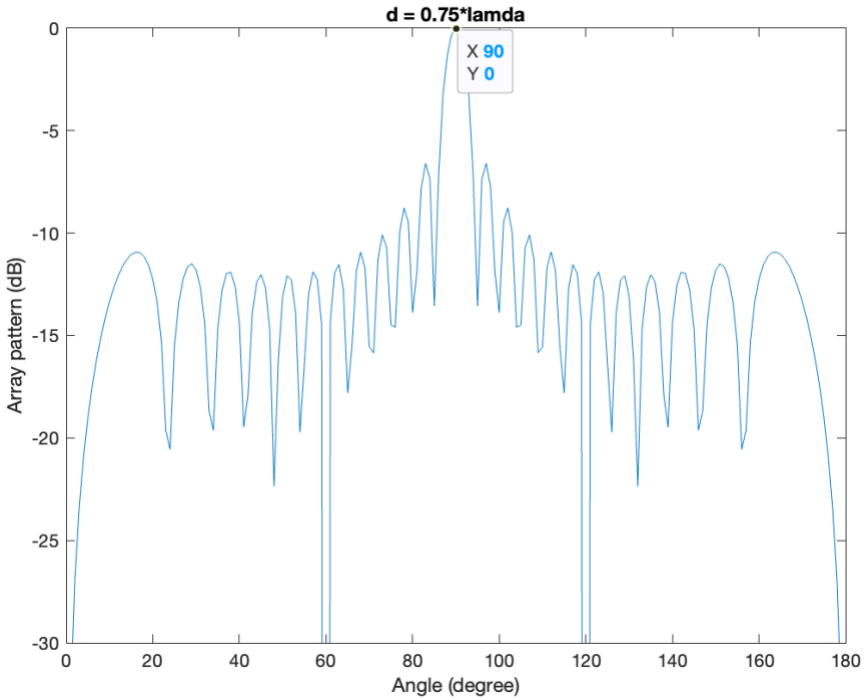

Figure 26. d = 0.75λ, Scan Angle = 90°

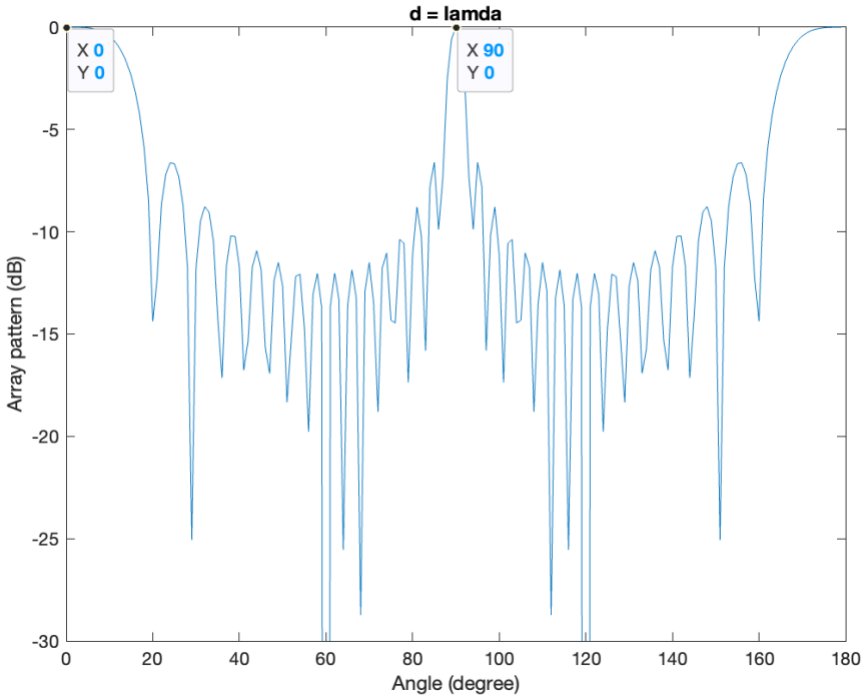

Figure 27. d = λ, Scan Angle = 90°

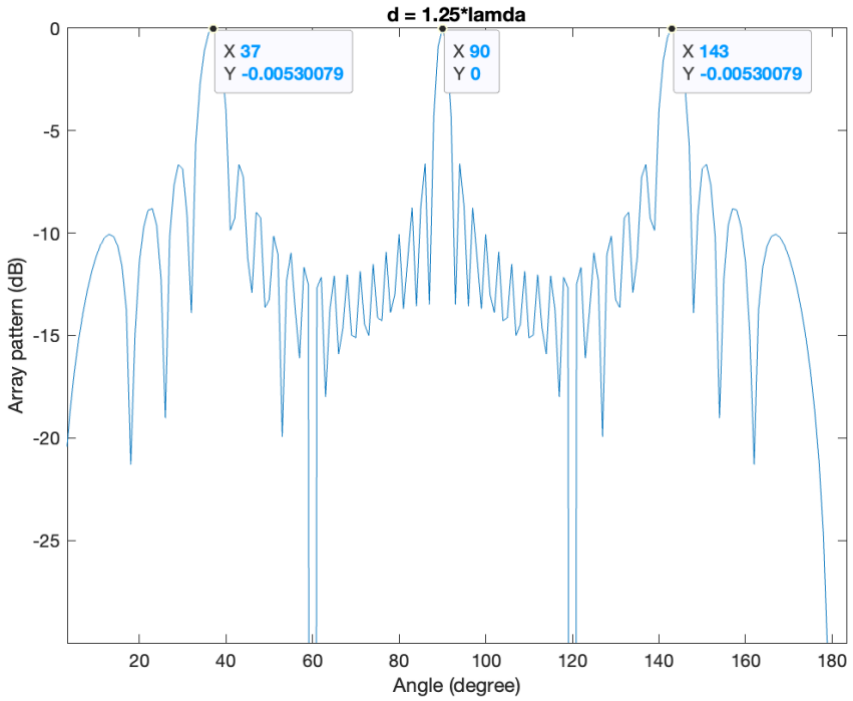

Figure 28. d = 1.25λ, Scan Angle = 90°

From the above figures, as d increases to and above λ, multiple beams with the same peak value occur. When d is at λ, there is one additional beam at 0°. When d is at 1.25λ, there are two additional beams at 37° and 143°.

Then apply a linear phase distribution to alter the scan angle θ_0 to 30° while keeping the rest of the parameters the same. The MATLAB simulation results are shown in Figure 29, Figure 30, Figure 31, Figure 32, and Figure 33.

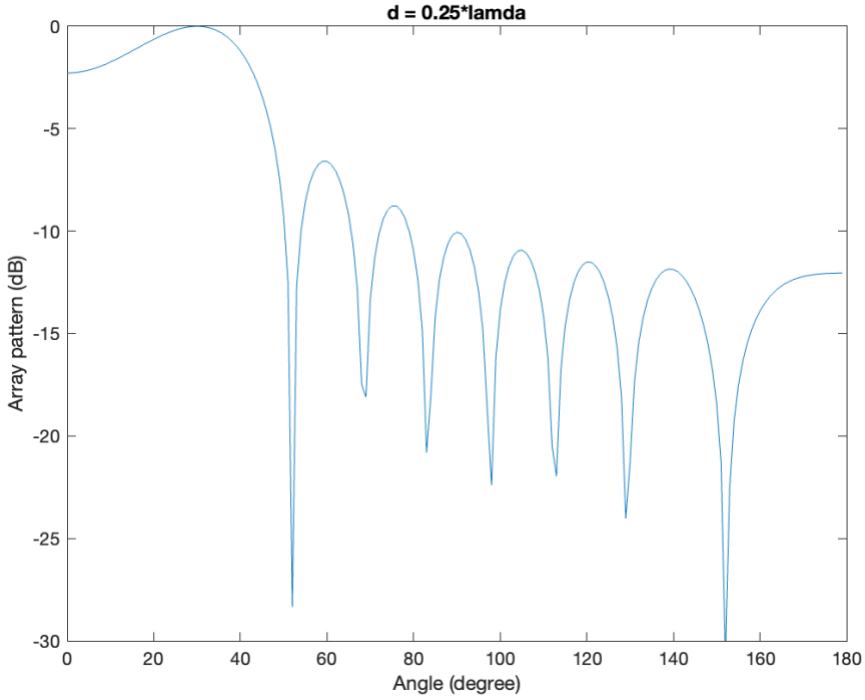

Figure 29. d = 0.25λ, Scan Angle = 30°

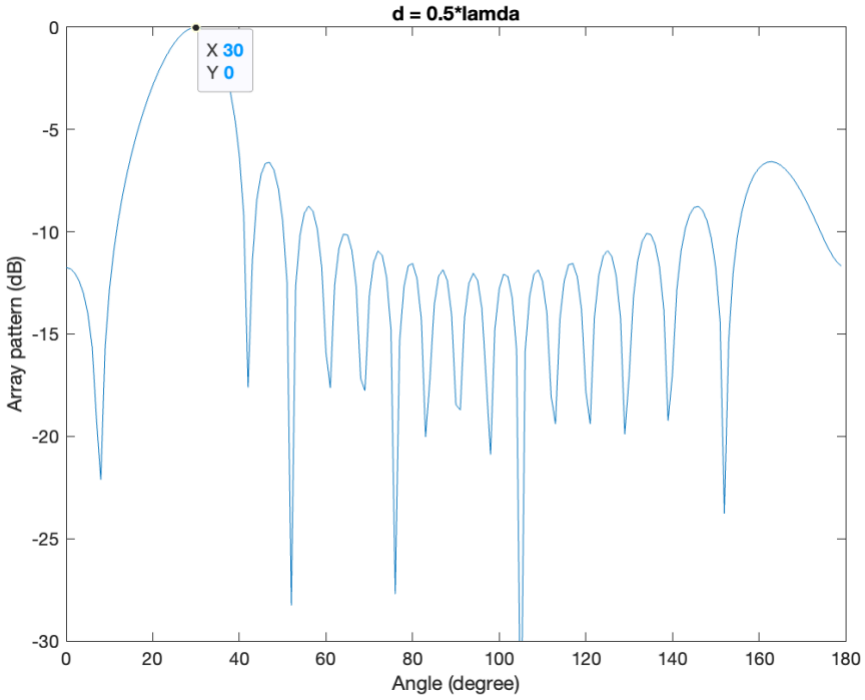

Figure 30. d = 0.5λ, Scan Angle = 30°

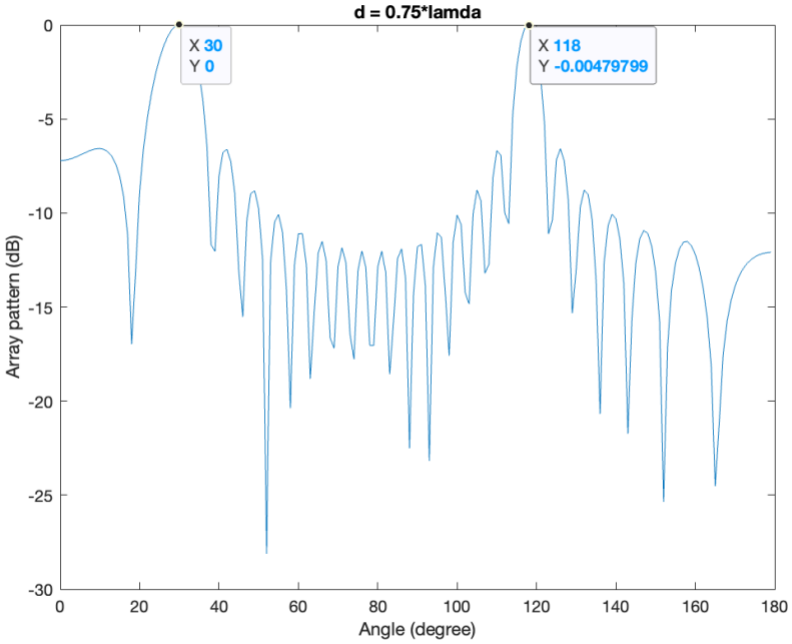

Figure 31. d = 0.75λ, Scan Angle = 30°

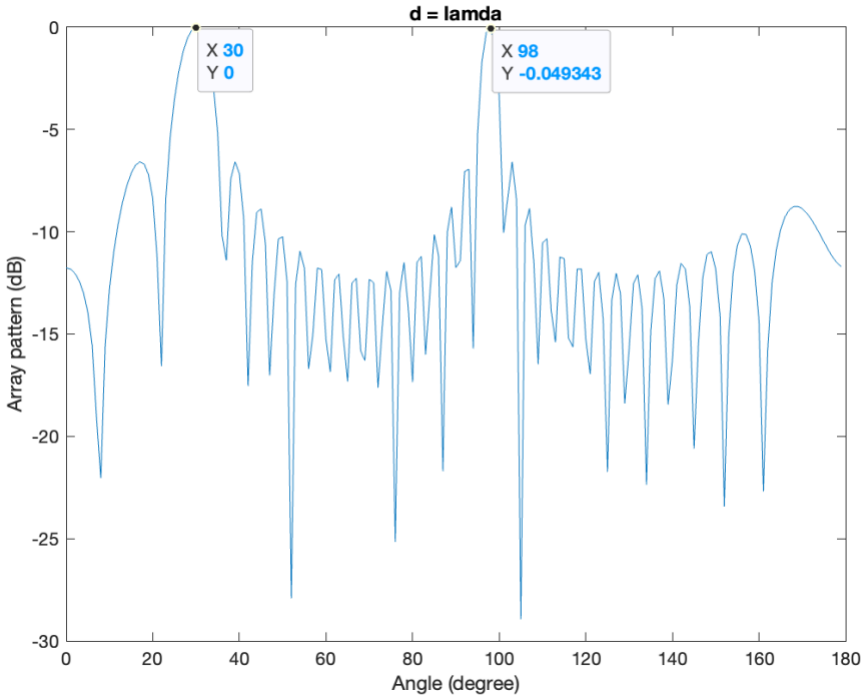

Figure 32 d = λ, Scan Angle = 30°

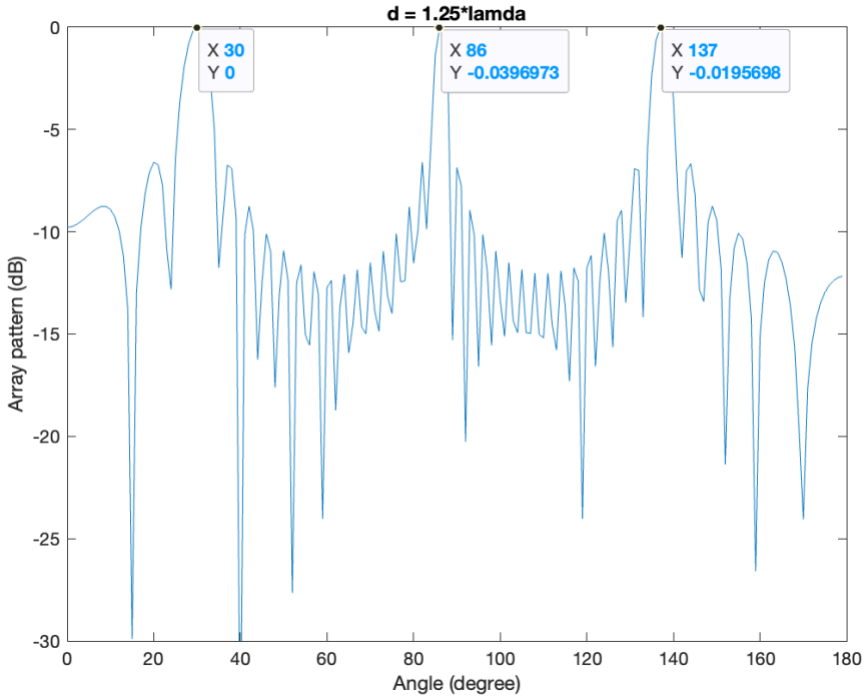

Figure 33. d = 1.25λ, Scan Angle = 30°

From the above figures, as d increases to and above 0.75λ, multiple beams with the same peak value occur. When d is at 0.75λ, there is one additional beam at 118°. When d is at λ, there is one additional beam at 98°. When d is at 1.25λ, there are two additional beams at 86° and 137°.

We can tell that as the distance between adjacent radiating elements d increases, the beamwidth of the main lobe (at 90°) narrows, which is an improvement. Another improvement is that the sidelobes shrink together. However, when d increases to a certain level, additional sidelobes with the same value of the main lobe appear. The occurrence of multiple beams is also confirmed in Chapter 3.3. This phenomenon is undesirable. And these additional sidelobes with the same value as the main lobe are grating lobes, produced by an array antenna when the inter-element spacing is sufficiently large to permit the in-phase addition of radiated fields in more than one direction [9].

5.2 Derivation of Grating Lobes

Considering a linear array with uniform amplitude and phase distribution, the phased difference between the fields radiated by adjacent elements is defined as

$$\gamma = kd\cos\theta = \frac{2\pi d}{\lambda}\cos\theta$$

So,

$$\cos\theta = \frac{\gamma\lambda}{2\pi d} = \frac{\gamma}{2\pi}\cdot\frac{\lambda}{d}$$

$$\theta = \cos^{-1}(\frac{\gamma}{2\pi}\cdot\frac{\lambda}{d})$$

Since the phase difference γ cycles every 2π, γ can be replaced with $\gamma + 2\pi m$, where $m = 0, \pm1, \pm2, \pm3, \ldots$

$$\theta = \cos^{-1}(\frac{2\pi m + \gamma}{2\pi}\cdot\frac{\lambda}{d})$$

Because

$$|\cos\theta| \leq 1$$

So,

$$\left|\frac{2\pi m + \gamma}{2\pi}\cdot\frac{\lambda}{d}\right| \leq 1$$

If we have more than one real number solution for the above equation when $m = 0, \pm 1, \pm 2, \pm 3, \ldots$, the grating lobes appear [10]. To avoid the occurrence of grating lobes, the equation can only have one real number solution for all m. The left side of the equation is at the minimum value when $m = 0$. When $m = 0$, the equation becomes

$$\left|\frac{\gamma}{2\pi} \cdot \frac{\lambda}{d}\right| \leq 1$$

$$\left|\frac{\gamma}{2\pi}\right| \cdot \left|\frac{\lambda}{d}\right| \leq 1$$

$$\left|\frac{\gamma}{2\pi}\right| \cdot \frac{\lambda}{d} \leq 1$$

$$\left|\frac{\gamma}{2\pi}\right| \leq \frac{d}{\lambda}$$

$$\frac{|\gamma|}{2\pi} \leq \frac{d}{\lambda}$$

Since

$$-\pi \leq \gamma \leq \pi$$

$$|\gamma| \leq \pi$$

$$\frac{|\gamma|}{2\pi} \leq \frac{1}{2}$$

The equation becomes

$$\frac{|\gamma|}{2\pi} \leq \frac{d}{\lambda} \leq \frac{1}{2}$$

So

$$d \leq \frac{\lambda}{2}$$

In conclusion, if the scan angle is between 0° and 180°, to avoid grating lobes, we must keep the distance between adjacent radiating elements d less or equal to $\frac{\lambda}{2}$, which is verified by the previous MATLAB stimulation.

Chapter 6

Beam Tapering

One of the major features of the phased array is beam tapering. By altering the amplitude distribution, the antenna sidelobes can be suppressed at some expense to the antenna gain and main lobe beamwidth, which is beam tapering.

Suppose that the number of radiating elements N is 16, the frequency f is 28 GHz, the distance between adjacent radiating elements d to 0.5λ, and the phase distribution is uniform. The radiation pattern by altering the amplitude distribution to uniform, Hamming window function, Taylor window function, and Hann window function are simulated by MATLAB (Appendix D) as shown in Figure 34, Figure 35, Figure 36, and Figure 37.

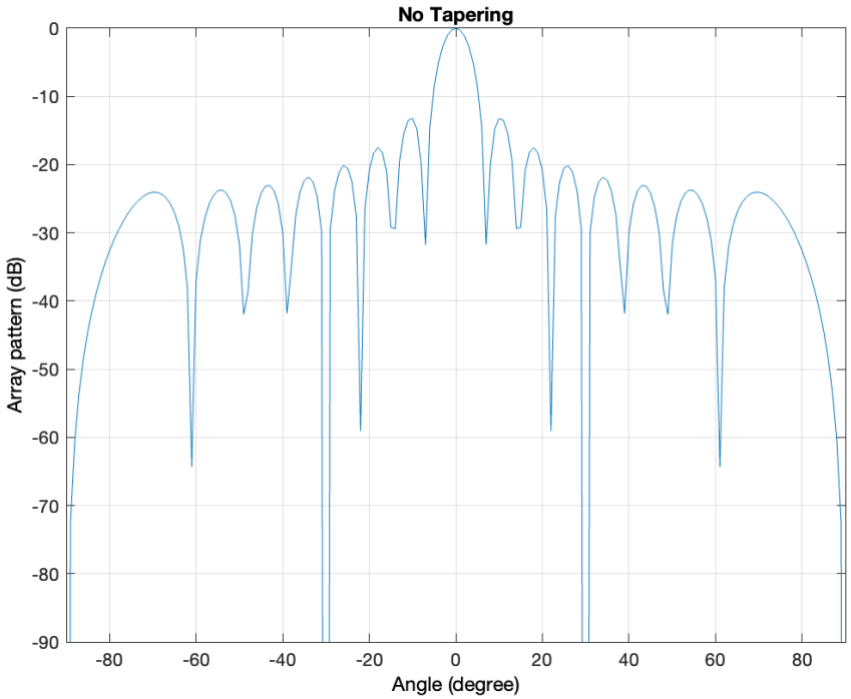

Figure 34. Uniform Amplitude Distribution

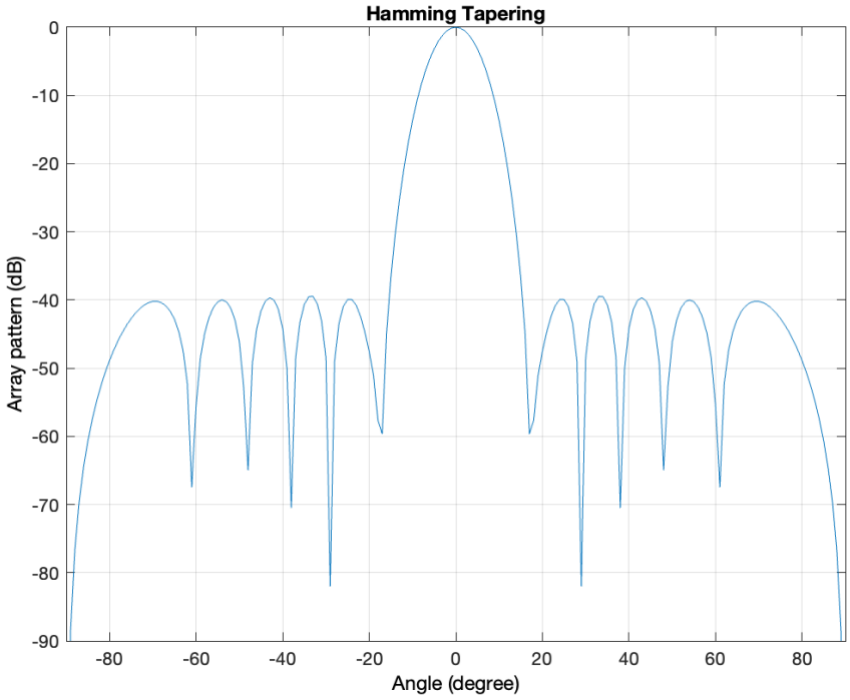

Figure 35. Hamming Tapering

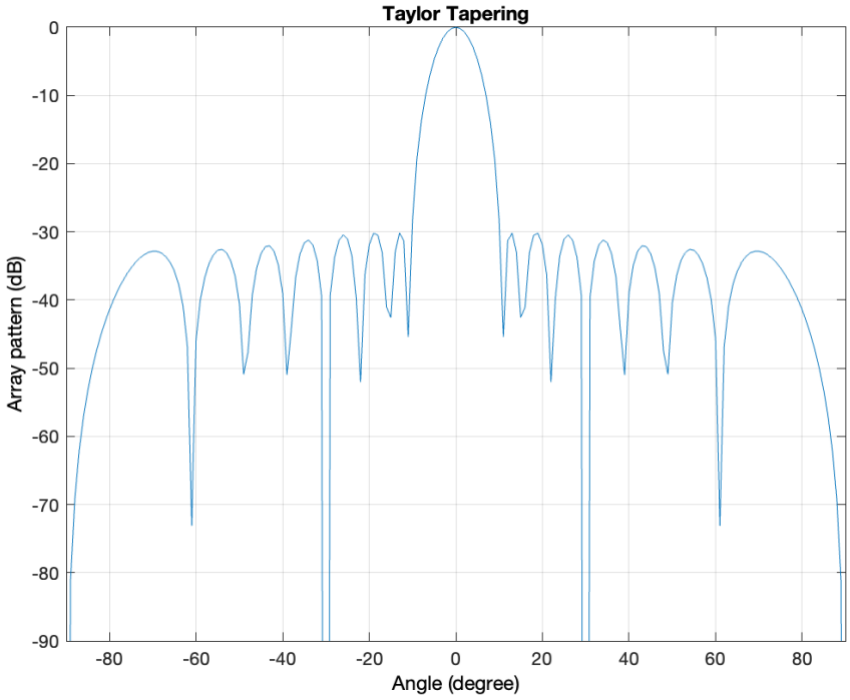

Figure 36. Taylor Tapering

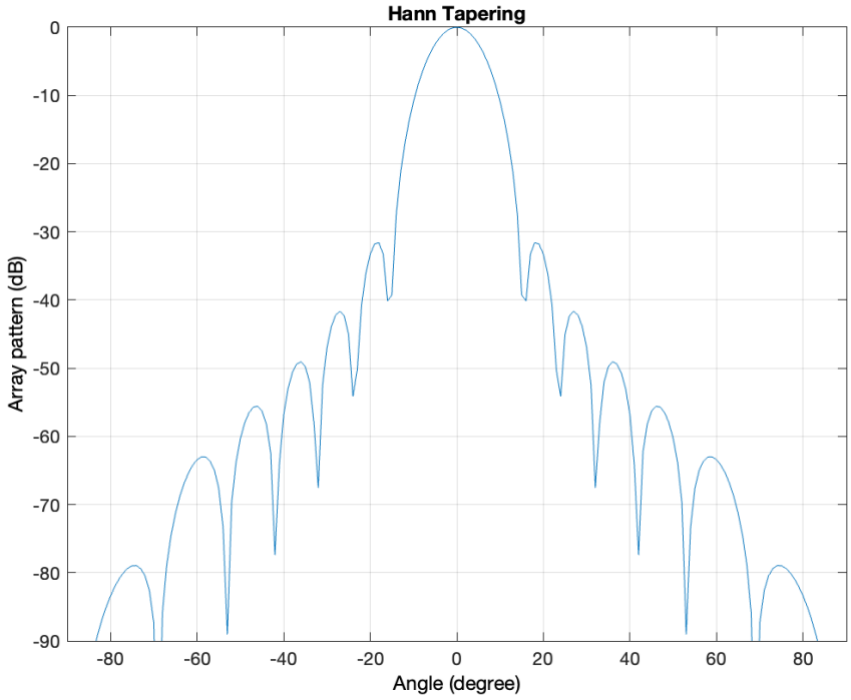

Figure 37. Hann Tapering

According to the above figures, beam tapering reduces sidelobes while increasing the beamwidth of the main lobe. Before applying an amplitude distribution, the sidelobes are mainly located between -10 dB to -30 dB. Hamming Tapering reduces sidelobes to -40 dB. Taylor Tapering decreases the sidelobes to between -30 dB and -40 dB. Hann Tapering reduces the sidelobes to less than -30 dB, which decreases more and more as moving toward the end-fire directions.

Chapter 7

Conclusion and Future Work

7.1 Conclusion

This thesis first introduces the development of communication technologies, the challenges involved in developing 5G technology, and the importance of the phased array in realizing 5G technology. It also presents the configuration of phased arrays and the derivation of array factors. It then used modeling, theoretical derivations, and MATLAB simulations to demonstrate beamforming, beam steering, and beam tapering, the three major features of the phased array. Rather than broadcasting in many directions, the phased array focuses on a concentrated beam, which is beamforming. By altering the phased distribution, the direction of the radiation pattern can be steered, which is beam steering. And the amplitude distribution controls the shape of the radiation pattern, which is beam tapering. This thesis also discusses the effect of grating lobes.

7.2 Future Work

In future research, I will continue working on beam tapering and find a better way to reduce the sidelobe levels while minimizing the reduction of directivity. The planar array and the frequency scanning array are two other common configurations that I will also explore their properties. Afterward, I will work on several challenges antenna engineers face in this field, including the scalability of phased arrays, the impact of component non-idealities on beamforming performance, and THz phased arrays.

Appendix A

```
%% Figure 6
clear
clc
theta = 1:180;
radiation_pattern = zeros(1,180);
plot(theta,radiation_pattern)
ylim([-30 5])
xlim([0 180])
xlabel('Angle (degree)')
ylabel('Amplitude (dB)')
title('Radiation Pattern of an Isotropic Radiating Element')

%% Figure 7
clear
clc
n = 2;
freq = 28*10e9;
c = physconst('LightSpeed');
lam = c/freq;
d = lam/2;
k = 2*pi/lam;

af = zeros(1,180);
```

```
for theta = 1:180
    for index = 0:n-1
        af(theta) = af(theta) +exp(1j*index*k*d*cos(deg2rad(theta)));
    end
    af(theta) = sqrt(abs(af(theta)));
end
theta = 1:180;
[max_value,max_index] = max(af);
plot(theta,mag2db(af/max_value))
ylim([-30 0])
xlim([0 180])
xlabel('Angle (degree)')
ylabel('Array pattern (dB)')
title('Radiation Pattern of a Linear Array with Uniform Amplitude and Phase Distribution')

%% Figure 8
clear
clc
n = 2;
freq = 28*10e9;
c = physconst('LightSpeed');
lam = c/freq;
d = lam/2;
k = 2*pi/lam;
norm_af = zeros(1,180);
```

```
for theta = 1:180
    norm_af(theta) =
sqrt(sin(n*pi*d*cos(deg2rad(theta))/lam))/(sqrt(n)*sqrt(sin(pi*d*cos(deg2rad(theta))/lam)));
end
theta = 1:180;
plot(theta,mag2db(norm_af))
ylim([-30 0])
xlim([0 180])
xlabel('Angle (degree)')
ylabel('Array pattern (dB)')
title('Radiation Pattern of a Linear Array with Uniform Amplitude and Phase Distribution')

%% Figure 9,10,11,12
clear
clc
freq = 28*10e9;
c = physconst('LightSpeed');
lam = c/freq;
k = 2*pi/lam;
% n = 4
n = 4;
af = zeros(1,180);
d = lam/2;
for theta = 1:180
    for index = 0:n-1
```

```
        af(theta) = af(theta) +exp(1j*index*k*d*cos(deg2rad(theta)));
    end
    af(theta) = sqrt(abs(af(theta)));
end
theta = 1:180;
[max_value,max_index] = max(af);
figure(1)
plot(theta,mag2db(af/max_value))
ylim([-30 0])
xlim([0 180])
xlabel('Angle (degree)')
ylabel('Array pattern (dB)')
title('N = 4')
% n = 8
n = 8;
af = zeros(1,180);
d = lam/2;
for theta = 1:180
    for index = 0:n-1
        af(theta) = af(theta) +exp(1j*index*k*d*cos(deg2rad(theta)));
    end
    af(theta) = sqrt(abs(af(theta)));
end
theta = 1:180;
[max_value,max_index] = max(af);
```

```
figure(2)
plot(theta,mag2db(af/max_value))
ylim([-30 0])
xlim([0 180])
xlabel('Angle (degree)')
ylabel('Array pattern (dB)')
title('N = 8')
% n = 16
n = 16;
af = zeros(1,180);
d = lam/2;
for theta = 1:180
    for index = 0:n-1
        af(theta) = af(theta) +exp(1j*index*k*d*cos(deg2rad(theta)));
    end
    af(theta) = sqrt(abs(af(theta)));
end
theta = 1:180;
[max_value,max_index] = max(af);
figure(3)
plot(theta,mag2db(af/max_value))
ylim([-30 0])
xlim([0 180])
xlabel('Angle (degree)')
ylabel('Array pattern (dB)')
```

```
title('N = 16')
% n = 32
n = 32;
af = zeros(1,180);
d = lam/2;
for theta = 1:180
    for index = 0:n-1
        af(theta) = af(theta) +exp(1j*index*k*d*cos(deg2rad(theta)));
    end
    af(theta) = sqrt(abs(af(theta)));
end
theta = 1:180;
[max_value,max_index] = max(af);
figure(4)
plot(theta,mag2db(af/max_value))
ylim([-30 0])
xlim([0 180])
xlabel('Angle (degree)')
ylabel('Array pattern (dB)')
title('N = 32')
%% Figure 13,14,15,1613
clear
clc
n = 2;
freq = 28*10e9;
```

```
c = physconst('LightSpeed');
lam = c/freq;
k = 2*pi/lam;
af = zeros(1,180);
% d = lam/2
d = lam/2;
for theta = 1:180
    for index = 0:n-1
        af(theta) = af(theta) +exp(1j*index*k*d*cos(deg2rad(theta)));
    end
    af(theta) = sqrt(abs(af(theta)));
end
theta = 1:180;
[max_value,max_index] = max(af);
figure(1)
plot(theta,mag2db(af/max_value))
ylim([-30 0])
xlim([0 180])
xlabel('Angle (degree)')
ylabel('Array pattern (dB)')
title('d = lam/2')
% d = 3*lam/2
d = 3*lam/2;
af = zeros(1,180);
for theta = 1:180
```

```
    for index = 0:n-1
        af(theta) = af(theta) +exp(1j*index*k*d*cos(deg2rad(theta)));
    end
    af(theta) = sqrt(abs(af(theta)));
end
theta = 1:180;
[max_value,max_index] = max(af);
figure(2)
plot(theta,mag2db(af/max_value))
ylim([-30 0])
xlim([0 180])
xlabel('Angle (degree)')
ylabel('Array pattern (dB)')
title('d = 3*lam/2')
% d = 5*lam/2
d = 5*lam/2;
af = zeros(1,180);
for theta = 1:180
    for index = 0:n-1
        af(theta) = af(theta) +exp(1j*index*k*d*cos(deg2rad(theta)));
    end
    af(theta) = sqrt(abs(af(theta)));
end
theta = 1:180;
[max_value,max_index] = max(af);
```

```
figure(3)
plot(theta,mag2db(af/max_value))
ylim([-30 0])
xlim([0 180])
xlabel('Angle (degree)')
ylabel('Array pattern (dB)')
title('d = 5*lam/2')
% d = 7*lam/2
d = 7*lam/2;
af = zeros(1,180);
for theta = 1:180
   for index = 0:n-1
      af(theta) = af(theta) +exp(1j*index*k*d*cos(deg2rad(theta)));
   end
   af(theta) = sqrt(abs(af(theta)));
end
theta = 1:180;
[max_value,max_index] = max(af);
figure(4)
plot(theta,mag2db(af/max_value))
ylim([-30 0])
xlim([0 180])
xlabel('Angle (degree)')
ylabel('Array pattern (dB)')
title('d = 7*lam/2')
```

Appendix B

```
%% figure 18,19,20,21,22,23
clear
clc
n = 16;
freq = 28*10e9;
c = physconst('LightSpeed');
lam = c/freq;
d = lam/2;
k = 2*pi/lam;
% scan_angle = 0
scan_angle = 0;
delta = k*d*cos(deg2rad(scan_angle));
af = zeros(1,180);
for theta = 0:179
   for index = 0:n-1
      af(theta+1) = af(theta+1) +exp(1j*index*(k*d*cos(deg2rad(theta))-delta));
   end
   af(theta+1) = sqrt(abs(af(theta+1)));
end
theta = 0:179;
[max_value,max_index] = max(af);
figure(1)
plot(theta,mag2db(af/max_value))
ylim([-30 0])
```

```
xlim([0 180])
xlabel('Angle (degree)')
ylabel('Array pattern (dB)')
title('scan angle = 0')
% scan_angle = 30deg
scan_angle = 30;
delta = k*d*cos(deg2rad(scan_angle));
af = zeros(1,180);
for theta = 1:180
    for index = 0:n-1
        af(theta) = af(theta) +exp(1j*index*(k*d*cos(deg2rad(theta))-delta));
    end
    af(theta) = sqrt(abs(af(theta)));
end
theta = 1:180;
[max_value,max_index] = max(af);
figure(2)
plot(theta,mag2db(af/max_value))
ylim([-30 0])
xlim([0 180])
xlabel('Angle (degree)')
ylabel('Array pattern (dB)')
title('scan angle = 30deg')
% scan_angle = 60deg
scan_angle = 60;
```

```
delta = k*d*cos(deg2rad(scan_angle));
af = zeros(1,180);
for theta = 1:180
    for index = 0:n-1
        af(theta) = af(theta) +exp(1j*index*(k*d*cos(deg2rad(theta))-delta));
    end
    af(theta) = sqrt(abs(af(theta)));
end
theta = 1:180;
[max_value,max_index] = max(af);
figure(3)
plot(theta,mag2db(af/max_value))
ylim([-30 0])
xlim([0 180])
xlabel('Angle (degree)')
ylabel('Array pattern (dB)')
title('scan angle =60deg')
% scan_angle = 90deg
scan_angle = 90;
delta = k*d*cos(deg2rad(scan_angle));
af = zeros(1,180);
for theta = 1:180
    for index = 0:n-1
        af(theta) = af(theta) +exp(1j*index*(k*d*cos(deg2rad(theta))-delta));
    end
```

```
    af(theta) = sqrt(abs(af(theta)));
end
theta = 1:180;
[max_value,max_index] = max(af);
figure(4)
plot(theta,mag2db(af/max_value))
ylim([-30 0])
xlim([0 180])
xlabel('Angle (degree)')
ylabel('Array pattern (dB)')
title('scan angle = 90deg')
% scan_angle = 120deg
scan_angle = 120;
delta = k*d*cos(deg2rad(scan_angle));
af = zeros(1,180);
for theta = 1:180
    for index = 0:n-1
        af(theta) = af(theta) +exp(1j*index*(k*d*cos(deg2rad(theta))-delta));
    end
    af(theta) = sqrt(abs(af(theta)));
end
theta = 1:180;
[max_value,max_index] = max(af);
figure(5)
plot(theta,mag2db(af/max_value))
```

```
ylim([-30 0])
xlim([0 180])
xlabel('Angle (degree)')
ylabel('Array pattern (dB)')
title('scan angle = 120deg')
% scan_angle = 150deg
scan_angle = 150;
delta = k*d*cos(deg2rad(scan_angle));
af = zeros(1,180);
for theta = 1:180
    for index = 0:n-1
        af(theta) = af(theta) +exp(1j*index*(k*d*cos(deg2rad(theta))-delta));
    end
    af(theta) = sqrt(abs(af(theta)));
end
theta = 1:180;
[max_value,max_index] = max(af);
figure(6)
plot(theta,mag2db(af/max_value))
ylim([-30 0])
xlim([0 180])
xlabel('Angle (degree)')
ylabel('Array pattern (dB)')
title('scan angle = 150deg')
```

Appendix C

```
%% Figure 24,25,26,27,28
clear
clc
n = 16;
freq = 28*10e9;
c = physconst('LightSpeed');
lam = c/freq;
k = 2*pi/lam;
scan_angle = 90;
% d = 0.25*lam
d = 0.25*lam;
delta = k*d*cos(deg2rad(scan_angle));
af = zeros(1,180);
for theta = 0:179
   for index = 0:n-1
      af(theta+1) = af(theta+1) +exp(1j*index*(k*d*cos(deg2rad(theta))-delta));
   end
   af(theta+1) = sqrt(abs(af(theta+1)));
end
theta = 0:179;
[max_value,max_index] = max(af);
figure(1)
plot(theta,mag2db(af/max_value))
ylim([-30 0])
```

```
xlim([0 180])
xlabel('Angle (degree)')
ylabel('Array pattern (dB)')
title('d = 0.25*lamda')
% d = 0.5*lam
d = 0.5*lam;
delta = k*d*cos(deg2rad(scan_angle));
af = zeros(1,180);
for theta = 0:179
    for index = 0:n-1
        af(theta+1) = af(theta+1) +exp(1j*index*(k*d*cos(deg2rad(theta))-delta));
    end
    af(theta+1) = sqrt(abs(af(theta+1)));
end
theta = 0:179;
[max_value,max_index] = max(af);
figure(2)
plot(theta,mag2db(af/max_value))
ylim([-30 0])
xlim([0 180])
xlabel('Angle (degree)')
ylabel('Array pattern (dB)')
title('d = 0.5*lamda')
% d = 0.75*lam
d = 0.75*lam;
```

```
delta = k*d*cos(deg2rad(scan_angle));
af = zeros(1,180);
for theta = 0:179
    for index = 0:n-1
        af(theta+1) = af(theta+1) +exp(1j*index*(k*d*cos(deg2rad(theta))-delta));
    end
    af(theta+1) = sqrt(abs(af(theta+1)));
end
theta = 0:179;
[max_value,max_index] = max(af);
figure(3)
plot(theta,mag2db(af/max_value))
ylim([-30 0])
xlim([0 180])
xlabel('Angle (degree)')
ylabel('Array pattern (dB)')
title('d = 0.75*lamda')
% d = lam
d = lam;
delta = k*d*cos(deg2rad(scan_angle));
af = zeros(1,180);
for theta = 0:179
    for index = 0:n-1
        af(theta+1) = af(theta+1) +exp(1j*index*(k*d*cos(deg2rad(theta))-delta));
    end
```

```
    af(theta+1) = sqrt(abs(af(theta+1)));
end
theta = 0:179;
[max_value,max_index] = max(af);
figure(4)
plot(theta,mag2db(af/max_value))
ylim([-30 0])
xlim([0 180])
xlabel('Angle (degree)')
ylabel('Array pattern (dB)')
title('d = lamda')
% d = 1.25*lam
d = 1.25*lam;
delta = k*d*cos(deg2rad(scan_angle));
af = zeros(1,180);
for theta = 0:179
    for index = 0:n-1
        af(theta+1) = af(theta+1) +exp(1j*index*(k*d*cos(deg2rad(theta))-delta));
    end
    af(theta+1) = sqrt(abs(af(theta+1)));
end
theta = 0:179;
[max_value,max_index] = max(af);
figure(5)
plot(theta,mag2db(af/max_value))
```

```
ylim([-30 0])

xlim([0 180])

xlabel('Angle (degree)')

ylabel('Array pattern (dB)')

title('d = 1.25*lamda')


%% Figure 29,30,31,32,33

clear

clc

n = 16;

freq = 28*10e9;

c = physconst('LightSpeed');

lam = c/freq;

k = 2*pi/lam;

scan_angle = 30;

% d = 0.25*lam

d = 0.25*lam;

delta = k*d*cos(deg2rad(scan_angle));

af = zeros(1,180);

for theta = 0:179

    for index = 0:n-1

        af(theta+1) = af(theta+1) +exp(1j*index*(k*d*cos(deg2rad(theta))-delta));

    end

    af(theta+1) = sqrt(abs(af(theta+1)));

end
```

```
theta = 0:179;
[max_value,max_index] = max(af);
figure(1)
plot(theta,mag2db(af/max_value))
ylim([-30 0])
xlim([0 180])
xlabel('Angle (degree)')
ylabel('Array pattern (dB)')
title('d = 0.25*lamda')
% d = 0.5*lam
d = 0.5*lam;
delta = k*d*cos(deg2rad(scan_angle));
af = zeros(1,180);
for theta = 0:179
    for index = 0:n-1
        af(theta+1) = af(theta+1) +exp(1j*index*(k*d*cos(deg2rad(theta))-delta));
    end
    af(theta+1) = sqrt(abs(af(theta+1)));
end
theta = 0:179;
[max_value,max_index] = max(af);
figure(2)
plot(theta,mag2db(af/max_value))
ylim([-30 0])
xlim([0 180])
```

```
xlabel('Angle (degree)')
ylabel('Array pattern (dB)')
title('d = 0.5*lamda')
% d = 0.75*lam
d = 0.75*lam;
delta = k*d*cos(deg2rad(scan_angle));
af = zeros(1,180);
for theta = 0:179
    for index = 0:n-1
        af(theta+1) = af(theta+1) +exp(1j*index*(k*d*cos(deg2rad(theta))-delta));
    end
    af(theta+1) = sqrt(abs(af(theta+1)));
end
theta = 0:179;
[max_value,max_index] = max(af);
figure(3)
plot(theta,mag2db(af/max_value))
ylim([-30 0])
xlim([0 180])
xlabel('Angle (degree)')
ylabel('Array pattern (dB)')
title('d = 0.75*lamda')
% d = lam
d = lam;
delta = k*d*cos(deg2rad(scan_angle));
```

```
af = zeros(1,180);
for theta = 0:179
    for index = 0:n-1
        af(theta+1) = af(theta+1) +exp(1j*index*(k*d*cos(deg2rad(theta))-delta));
    end
    af(theta+1) = sqrt(abs(af(theta+1)));
end
theta = 0:179;
[max_value,max_index] = max(af);
figure(4)
plot(theta,mag2db(af/max_value))
ylim([-30 0])
xlim([0 180])
xlabel('Angle (degree)')
ylabel('Array pattern (dB)')
title('d = lamda')
% d = 1.25*lam
d = 1.25*lam;
delta = k*d*cos(deg2rad(scan_angle));
af = zeros(1,180);
for theta = 0:179
    for index = 0:n-1
        af(theta+1) = af(theta+1) +exp(1j*index*(k*d*cos(deg2rad(theta))-delta));
    end
    af(theta+1) = sqrt(abs(af(theta+1)));
```

```
end

theta = 0:179;

[max_value,max_index] = max(af);

figure(5)

plot(theta,mag2db(af/max_value))

ylim([-30 0])

xlim([0 180])

xlabel('Angle (degree)')

ylabel('Array pattern (dB)')

title('d = 1.25*lamda')
```

Appendix D

```
%% Figure 34
Array = phased.ULA('NumElements',16,...
    'ArrayAxis','z');
Array.ElementSpacing = 0.5*0.0107142857142857;
Array.Taper = ones(1,16).';
Elem = phased.IsotropicAntennaElement;
Elem.FrequencyRange = [0 28000000000];
Array.Element = Elem;
Frequency = 28000000000;
PropagationSpeed = 300000000;
w = ones(getNumElements(Array), length(Frequency));
format = 'rectangular';
cutAngle = 0;
plotType = 'PowerDB';
plotStyle = 'Overlay';
figure;
pattern(Array, Frequency, cutAngle, -90:90, 'PropagationSpeed', PropagationSpeed,...
    'CoordinateSystem', format ,'weights', w, ...
    'Normalize', true,...
    'Type', plotType, 'PlotStyle', plotStyle);
ylim([-90 0])
xlim([-90 90])
xlabel('Angle (degree)')
ylabel('Array pattern (dB)')
```

```
title('No Tapering')


%% Figure 35
Array = phased.ULA('NumElements',16,...
    'ArrayAxis','z');
Array.ElementSpacing = 0.5*0.0107142857142857;
Array.Taper = hamming(16);
Elem = phased.IsotropicAntennaElement;
Elem.FrequencyRange = [0 28000000000];
Array.Element = Elem;
Frequency = 28000000000;
PropagationSpeed = 300000000;
w = ones(getNumElements(Array), length(Frequency));
format = 'rectangular';
cutAngle = 0;
plotType = 'PowerDB';
plotStyle = 'Overlay';
figure;
pattern(Array, Frequency, cutAngle, -90:90, 'PropagationSpeed', PropagationSpeed,...
    'CoordinateSystem', format ,'weights', w, ...
    'Normalize', true,...
    'Type', plotType, 'PlotStyle', plotStyle);
ylim([-90 0])
xlim([-90 90])
xlabel('Angle (degree)')
```

```
ylabel('Array pattern (dB)')

title('Hamming Tapering')


%% Figure 37

Array = phased.ULA('NumElements',16,...

   'ArrayAxis','z');

Array.ElementSpacing = 0.5*0.0107142857142857;

Array.ElementSpacing = 0.5*0.0107142857142857;

Array.Taper = hann(16);

Elem = phased.IsotropicAntennaElement;

Elem.FrequencyRange = [0 28000000000];

Array.Element = Elem;

Frequency = 28000000000;

PropagationSpeed = 300000000;

w = ones(getNumElements(Array), length(Frequency));

format = 'rectangular';

cutAngle = 0;

plotType = 'PowerDB';

plotStyle = 'Overlay';

figure;

pattern(Array, Frequency, cutAngle, -90:90, 'PropagationSpeed', PropagationSpeed,...

   'CoordinateSystem', format ,'weights', w, ...

   'Normalize', true,...

   'Type', plotType, 'PlotStyle', plotStyle);

ylim([-90 0])
```

```
xlim([-90 90])

xlabel('Angle (degree)')

ylabel('Array pattern (dB)')

title('Hann Tapering')
```

BIBLIOGRAPHY

[1] Mutabazi, Patrick. *The Mobile Wireless Communication Technology Journey - 0G, 1G, 2G, 3G, 4G, 5G*. LinkedIn, 6 Feb. 2021, https://www.linkedin.com/pulse/mobile-wireless-communication-technology-journey-0g-mutabazi/.

[2] Banday, Yusra, et al. *Effect of Atmospheric Absorption on Millimetre Wave Frequencies for 5G Cellular Networks.* IET Communications, vol. 13, no. 3, 2019.

[3] El-Shorbagy, Abdel-moniem. *5G Technology and the Future of Architecture.* Procedia Computer Science, vol. 182, 2021.

[4] Nordrum, Amy, et al. *Everything You Need to Know About 5G.* IEEE Spectrum, 9 Sept. 2021, https://spectrum.ieee.org/everything-you-need-to-know-about-5g.

[5] *Disruptive Beamforming Trends Improving Mmwave 5G.* GSA, 5 Jan. 2021, https://gsacom.com/paper/disruptive-beamforming-trends-improving-mmwave-5g/.

[6] *Phased Array Antennas: Principles, Advantages, and Types.* Cadence System Analysis, 22 Sept. 2021, https://resources.system-analysis.cadence.com/blog/msa2021phased-array-antennas-principles-advantages-and-types.

[7] *Phased Array Antennas: Principles, Advantages, and Types.* Cadence System Analysis, 22 Sept. 2021, https://resources.system-analysis.cadence.com/blog/msa2021phased-array-antennas-principles-advantages-and-types.*The near-Field vs. Far-Field Regions of an Antenna.* Cadence, 4 Nov. 2021, https://resources.system-analysis.cadence.com/blog/msa2021-the-near-field-vs-far-field-regions-of-an-antenna.

[8] Ulaby, Fawwaz T., and Umberto Ravaioli. *Fundamentals of Applied Electromagnetics*. Pearson, 2015.

[9] *145-2013 - IEEE Standard for Definitions of Terms for Antennas.* IEEE Xplore, https://ieeexplore.ieee.org/document/6758443.

[10] Delos, Peter, et al. *Phased Array Antenna Patterns-Part 2: Grating Lobes and Beam Squint.* Analog Devices, https://www.analog.com/en/analog-dialogue/articles/phased-array-antenna-patterns-part2.html.

ACADEMIC VITA

ANG CHEN
cdchenang@gmail.com

EDUCATION

Schreyer Honors College, **The Pennsylvania State University**, University Park, PA August 2022
Bachelor of Science in Electrical Engineering (Honors and Distinction), minor in Mathematics

PROFESSIONAL EXPERIENCE

Undergraduate Research Assistant Jan 2021 – Present
Supervised by Dr. Wooram Lee, College of Engineering, The Pennsylvania State University
- Conducted research on the properties of beam steering, beam tapering, grating lobes, and beam squint
- Designed a MATLAB program to realize the radiation pattern of phased arrays
- Wrote an undergraduate honors thesis on modeling, theory, and simulation of wideband phased arrays

Undergraduate Research Assistant Jan 2022 – May 2022
Supervised by Dr. Xiaozhen Wang, College of Engineering, The Pennsylvania State University
- Designed a project to display the local time on an LCD screen by communicating a microcontroller with a GPS receiver via UART
- Realized a finite state machine for a Thermostat by discrete logic
- Realized a finite state machine for a Thermostat by myDAQ and LabVIEW
- Realized a finite state machine for a Thermostat by embedded microcontroller and C
- Realized a finite state machine for a Thermostat by Programmable logic device and HDL

Teaching Assistant of Mathematics and Statistics Aug 2020 – Jun 2021
Rutgers University & Council on International Educational Exchange
- Prepared and delivered interactive questions and activities during recitation sections
- Evaluated student performance, including grading exams, quizzes, and assignment
- Maintained weekly office hours to communicate in person with students
- Met with the course instructor to discuss course-related issues and to determine grading criteria
- Attended lecture sessions and recorded detailed notes of in-class lectures

Undergraduate Research Assistant Nov 2019 – Feb 2020
Supervised by Dr. Sarah Ritter, College of Engineering, The Pennsylvania State University
- Collected and categorized traffic data from the local government
- Analyzed and developed ways to improve the local traffic efficiency
- Collaborated with Texas Instruments to encoded robots with different functions
- Designed a robotic autonomous bus powered by solar energy

Undergraduate Research Assistant Aug 2019 – Nov 2019
Supervised by Dr. Sarah Ritter, College of Engineering, The Pennsylvania State University
- Researched to find the reasons for the water crisis in Ethiopia
- Collected data on the functionalities of water purification devices on sale
- Conducted tests to compare filtering performances of different materials
- Designed a model for a portable water reservoir with filters

SKILLS

Python, C, SolidWorks, MATLAB, Multisim, LabVIEW, FPGA, ADS, WinCUPL, cRIO, MPLAB, PuTTy, Microcontroller

LEADERSHIP AND INVOLVEMENT

Secretary, Chinese Students and Scholars Association, The Pennsylvania State University Sep 2018 – May 2022
- Campaigned on issues that affect international students at Penn State
- Represented and advocated the views of international students at Penn State
- Held academic and career events for international students
- Held Pre-Departure Orientation with Penn State Global in Asia

- Led the strategic development of the organization
- Led the organization's executive team to ensure effective working

Program Coordinator, Penn State Global, The Pennsylvania State University Aug 2020 – Jun 2021
- Developed and maintained the partnership with Chinese universities and the U.S. Embassy in China
- Designed and held in-person academic and co-curricular events in China
- Connected Penn State alumni in China with Penn State
- Promoted Penn State in China by creating flyers, brochures, videos, and updating social media
- Coordinated with Global Penn State in the preparation, implementation, and evaluation of various programs
- Documented programs, event pictures, and survey feedback

Member, Chinese Student Council, The Pennsylvania State University Sep 2019 – Present
Member, Eta Kappa Nu Electrical Engineering Honor Society (IEEE-HKN) Sep 2019 – Present
Member, Institute of Electrical and Electronics Engineers (IEEE) Sep 2019 – Present

WORK EXPERIENCE

Development Intern, China Telecom Americas Sep 2019 – Jan 2022
Resident Assistant, The Pennsylvania State University Aug 2020 – Feb 2021
Auxiliary Police Officer, University Police, The Pennsylvania State University Oct 2018 – Aug 2021

AWARDS AND HONORS

The John W. Oswald Award, The Pennsylvania State University 2022
The Partisan Award, The Pennsylvania State University 2022
Kelly E. and Justin L. Becker Scholarship, The Pennsylvania State University 2022
Schreyer Honors College Scholarship, The Pennsylvania State University 2022
Schreyer Scholar, The Pennsylvania State University 2020-2022
Dean's List, The Pennsylvania State University 2018-2022
The Ardeth and Norman Frisbey International Student Award, The Pennsylvania State University 2021
The John and Veda Black Award, The Pennsylvania State University 2021
Penn State First Student Leadership Award, The Pennsylvania State University 2021
Summer Success Scholarship Award, The Pennsylvania State University 2019-2020